1951

Design of pneumatic strain gage and its use in measuring deformation of small gage wire.

Laessle, Frank Willard

Monterey, California: U.S. Naval Postgraduate School

DESIGN OF PNEUMATIC STRAIN GAGE AND ITS USE IN MEASURING DEFORMATION OF SMALL GAGE WIRE

BY

F. W. LAESSLE

DESIGN OF PNEUMATIC STRAIN GAGE AND ITS USE IN MEASURING DEFORMATION OF SMALL GAGE WIRE

-

F. W. Laessle

DESIGN OF PNEUMATIC STRAIN GAGE AND ITS USE IN MEASURING DEFORMATION OF SMALL GAGE WIRE

by

Frank Willard Laessle,
Lieutenant, United States Navy

Submitted in partial fulfillment
of the requirements
for the degree of
MASTER OF SCIENCE
in
MECHANICAL ENGINEERING

United States Naval Postgraduate School
Annapolis, Maryland
1951

This work is accepted as fulfilling
the thesis requirements for the degree of
MASTER OF SCIENCE
in
MECHANICAL ENGINEERING

from the
United States Naval Postgraduate School.

PREFACE

In the field of engineering, there is always present the need for obtaining more precision in small measurements, and at the same time attaining this end by simple and versatile means.

In order to detect and register very small dimensional changes brought about in a stressed elastic material, instrumentation must be designed and built to incorporate great sensitivity which is attained in large part by utilizing some form of magnification, to enlarge upon the actual change and make the measurement readable.

In the work to follow, the problem of measuring transverse and longitudinal strains set up in small diameter wire under tension, as a means of obtaining reliable values of Poisson's ratio for the material, is taken up and a means of obtaining results is described.

Determinations of the longitudinal strains existing is accomplished by conventional optical methods, while that of obtaining the transverse strain was resolved by application of the principle of so-called pneumatic amplification.

The considerations arising in the design of two pneumatic strain gages, their calibration and the design of a tension producer are discussed together with results of tests undertaken with this equipment.

The designs for the first pneumatic strain gage and tension producer were begun in December 1950 and were built and completed by the U. S. Naval Experiment Station in

April 1951. The second strain gage was designed to eliminate certain fabrication deficiencies found in the first; it was manufactured in the School's machine shop.

The gages were calibrated at the Naval Postgraduate School, using an interferometer and pressure control equipment designed by Professor G. H. Lee and Instructor I. H. Stockel who were working in an allied field. Following the calibration of the gage, several strain measurements were made on .125 inch wire and Poisson's ratio determined for comparison with existing data for the material.

I wish to express my appreciation to Professor G. H. Lee for his suggestions and guidance throughout the project and to Professor E. K. Gatcomb for his aid in consummating the mechanical design features of the piston-type gage. Thanks are also due my fellow students and Joseph Octavec of the School's machine shop for his efforts in eliminating operational troubles and in producing one of the gages.

TABLE OF CONTENTS

LIST OF ILLUSTRATIONS

TABLE OF SYMBOLS AND ABBREVIATIONS

		Dimensions
α	- Dimensionless ratio s/D_2	
A_1	- Primary fixed orifice area	L^2
A_2	- Secondary variable orifice tip circumferential gap area	L^2
β	- Dimensionless ratio D_2/D_1	
C_d	- Coefficient of discharge	
C_u	- Correction for initial velocity	
δ	- Total elongation	L
D_1	- Primary fixed orifice diameter	L
D_2	- Secondary variable orifice tip inside diameter	L
E	- Young's modulus of elasticity	M/LT^2
ϵ_L	- Unit strain, longitudinally	
ϵ_T	- Unit strain, transversely	
H	- Supply pressure head (inches of water)	L
h	- Intermediate pressure head between orifice 1 and 2 (inches of water)	L
h_o	- Reading of manometric column with exit of intermediate chamber open	
h_c	- Reading of manometric column with exit of intermediate chamber closed.	
h_m	- Reading of manometric column corresponding to maximum magnification or equal to 3/4H.	
h_1	- Reading of manometer corresponding to a gage setting s_1 on left of maximum point	
h_2	- Reading of manometer corresponding to a gage setting s_2 on right of maximum point.	

		Dimensions
k	- $\frac{Cp}{Cv}$ ratio of specific heat at constant pressure to the specific heat at constant volume	
λ	- Wave length of light source	L
L	- Tension producer loading lever arm	L
μ	- Poisson's ratio	
M_α	- Magnification $\frac{dh}{d\alpha}$	
M'	- Mass rate of flow	$\frac{M}{T}$
M_s	- Magnification $\frac{dh}{ds}$	
m	- Increment mass of fluid under consideration	M
ω	- Sensitivity	
P	- Pressure force per unit area	M/T^2L
p	- Pressure force per unit area, $= \frac{P}{g'}$ where g' is numerically equal to the acceleration due to gravity	$\frac{M}{T^2L}$
Q	- Volume rate of flow	L^3/T
ρ	- Mass density	$\frac{M}{L^3}$
R	- Tension producer wire pulling arm	L
σ	- Stress	M/LT^2
s	- Gap clearance	L
"Solex"	- Name given to constant pressure controlling source	
U	- Velocity	L/T
V	- Volume of $\underline{m}$ at any instant	L^3
W	- Tension producer load	ML/T^2
Z	- Potential head	L

INTRODUCTION

Pneumatic amplification actually is a means of capitalizing on the properties of a flowing gas which are at all times such as to fulfill the laws of conservation of energy and continuity of mass. If within the boundaries of a flowing fluid, the sectional area is reduced, then in order that continuity of mass be maintained, the velocity must increase. Associated with the velocity increase and again in keeping with energy conservation, there is a pressure decrease. It follows that the existing pressure is proportional to the section area.

I - DESIGN CONSIDERATIONS

1 - Application of Flow Theory to Strain Gage System

Applying the principles set forth in the introduction to the pneumatic strain gage, together with equation

$$h = \frac{H}{1 + \frac{16D_2^2 s^2}{D_1^4}} \qquad (1)$$

developed in Appendix "A" for a similar situation, Figure 18, a convenient method of measuring deformation can be realized. Figure 1 represents one such system, and the particular arrangement used in measuring transverse strain of small diameter wire.

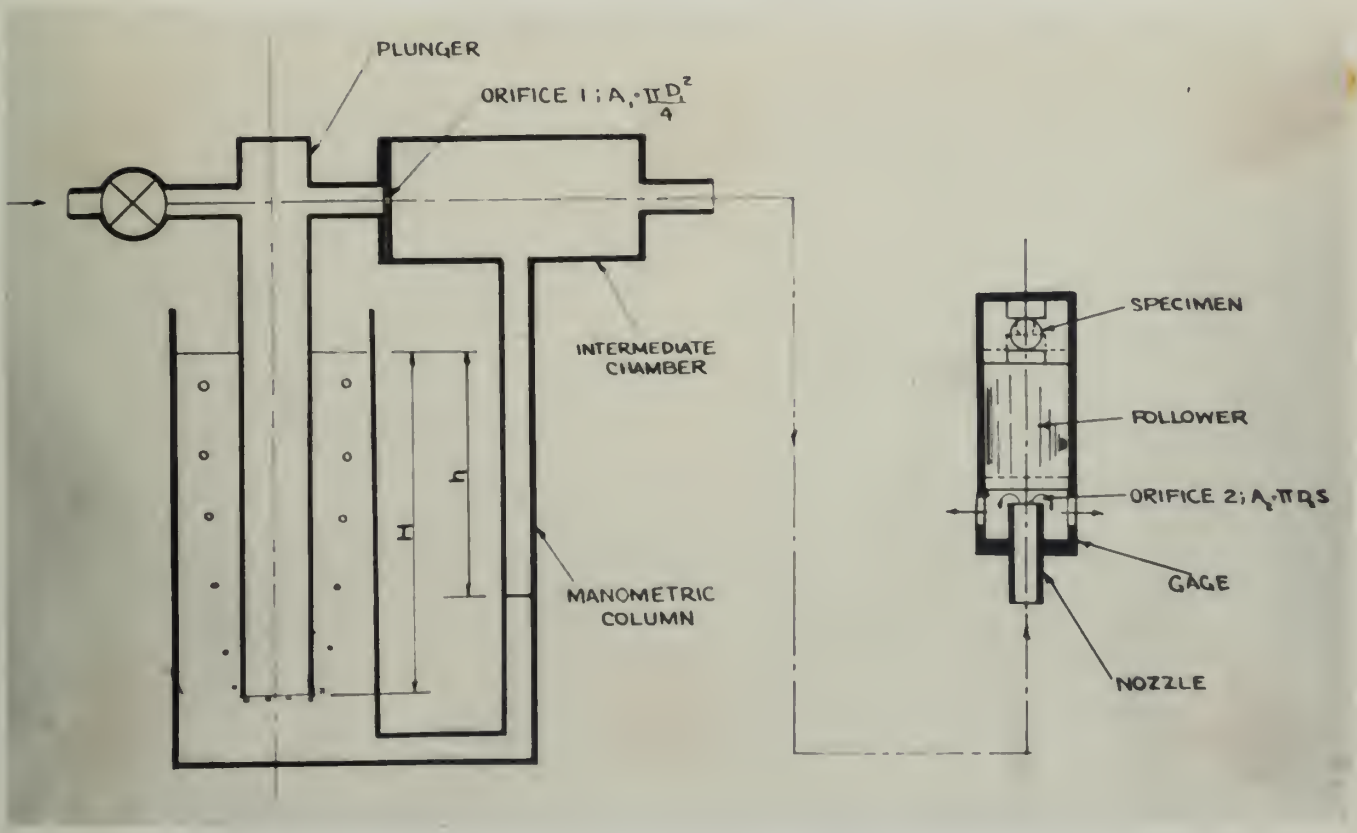

Figure 1 - Schematic of strain gage system.

Referring to Figure 1, air under low pressure is supplied from the left through a valve into the pressure controlling device "Solex" which maintains the initial pressure P_1 at H inches of water in the plunger and in the space between the valve and the first orifice A_1. To the right of A_1 the pressure h is controlled by the amount that the gage variable orifice A_2 is open. When A_2 is closed, h will equal H and the water level in the manometric column will be at its low point. If it were possible to open A_2 all the way back at the manifold, it is evident that h would be 0 gage or atmospheric pressure. In use h will be between 0 and H and generally $3/4H$, as will be shown later.

At the gage, it can be seen that as the diameter of the specimen decreases, the piston follower will rise and increase the gap s between A_2 and the lower face of the piston. This will result in a decrease in h and the water column will rise.

In the system just described, we have then, two orifices. A_1 fixed and A_2 variable. The pressure entering A_1 is H, leaving A_1 and entering A_2 is h, and leaving A_2 is atmospheric. It can be seen that the pressure prevailing between A_1 and A_2 is a function of A_1 and A_2. With A_1 fixed and A_2 variable, the pressure h then is a measure of the size of orifice A_2.

For reasons that will become apparent later on, it becomes convenient to use the following notation:

$$\alpha = \frac{s}{D_2} \qquad \text{and} \qquad \beta = \frac{D_2}{D_1}$$

Then equation (1) becomes:

$$h = \frac{H}{1 + 16\beta^4\alpha^2} \tag{2}$$

Equations (1) and (2) then define $\underline{h}$ as a function of $\underline{s}$, $\underline{D}_2$ and $\underline{D}_1$, all independent, to give equality of mass flow through orifices 1 and 2. $\underline{D}_1$ and $\underline{D}_2$ become and remain constants after being assigned certain values, leaving $\underline{s}$ as the independent variable. $\frac{dh}{d\alpha}$ is proportional to the magnification $\frac{dh}{ds}$ by the factor $\underline{D}_2$, i.e., $\frac{1}{D_2}\frac{dh}{d\alpha} = \frac{dh}{ds} = M_s$ so that the characteristics of $\frac{dh}{d\alpha}$ or M_α when plotted will be similar to $\frac{dh}{ds}$ for a given $\underline{D}_2$.

Therefore, taking the derivative of (2) with respect to α :

$$h' \text{ or } \frac{dh}{d\alpha} = \frac{-32\beta^4\alpha H}{(1 + 16\beta^4\alpha^2)^2} \tag{3}$$

With $h_{(max)}$ at $\alpha = 0$

$$h'' \text{ or } \frac{d^2h}{d\alpha^2} = 32\beta^4 H\left[\frac{48\beta^4\alpha^2 - 1}{(1 + 16\beta^4\alpha^2)^3}\right] \tag{4}$$

With $\frac{dh}{d\alpha}(max)$ at $\alpha = \frac{1}{4\sqrt{3}\beta^2} = \frac{.1445}{\beta^2}$

$$h''' \text{ or } \frac{d^3h}{d\alpha^3} = \frac{-6144\beta^8 H\alpha(16\beta^4\alpha^2 - 1)}{(1 + 16\beta^4\alpha^2)^4} \tag{5}$$

With $\frac{d^2h}{d\alpha^2}(max)$ at $\alpha = \frac{1}{4\beta^2}$ and $\frac{d^2h}{d\alpha^2}(min)$ at $\alpha = 0$

$$h^{iv} \text{ or } \frac{d^4h}{d\alpha^4} = \frac{6144\beta^8 H\left[1280\beta^8\alpha^4 - 160\beta^4\alpha^2 + 1\right]}{(1 + 16\beta^4\alpha^2)^5} \tag{6}$$

With $\frac{d^3h}{d\alpha^3}(max)$ at $\alpha = \frac{.344}{\beta^2}$ and $\frac{d^3h}{d\alpha^3}(min)$ at $\alpha = \frac{.082}{\beta^2}$

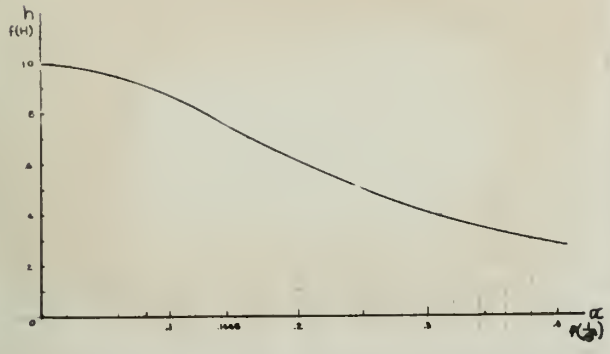

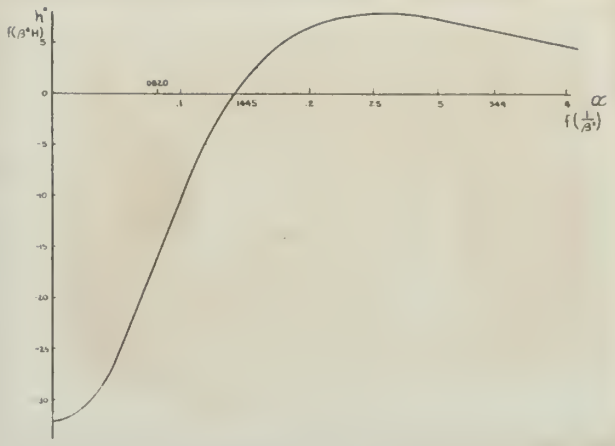

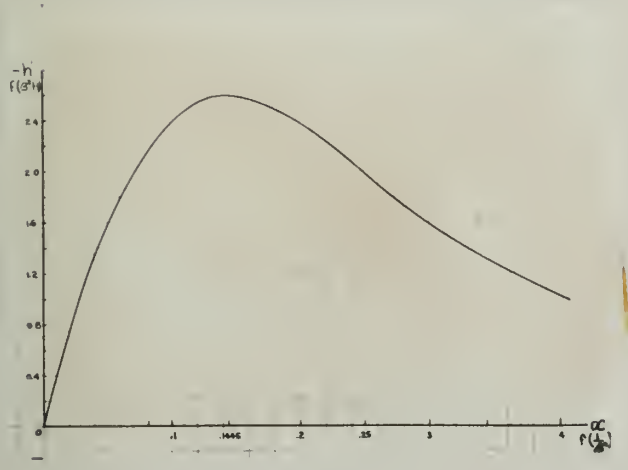

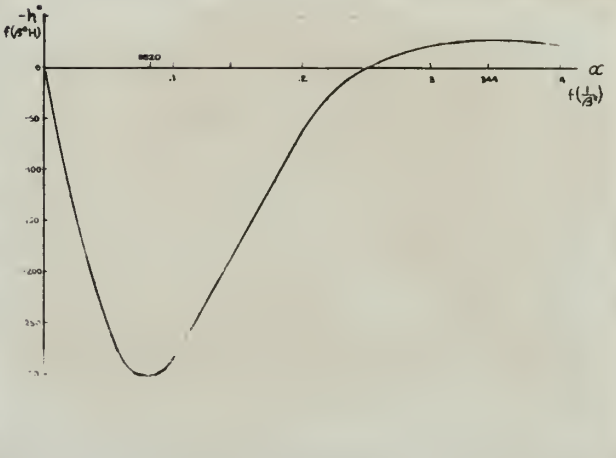

Figure 2-a,b,c and d - Function characteristics

Plots of $\underline{h}$, $\underline{h}'$, $\underline{h}''$ and $\underline{h}'''$ appear as Figure 2-a, b,c and d. From Figure 2 the following can be deduced:

a - Maximum magnification occurs at $\alpha = \frac{.1445}{\beta^2}$. Since $\underline{h}''_\alpha$ is zero at this point and the curvature of $\underline{h}'_\alpha$ as indicated by $\underline{h}'''_\alpha$ is negative in the vicinity of this point.

b - Approximate linearity of $\underline{h}$ and α occurs at this point and vicinity as indicated by $\underline{h}''_\alpha$ being zero at $\alpha = \frac{.1445}{\beta^2}$ showing inflection of the $\underline{h}_\alpha$ curve, with negative curvature to the left and positive curvature to the right.

c - That this point and vicinity is the most desirable condition to design for.

d - In terms of $\frac{dh}{ds}$ and s

Realize that $$\frac{dh}{ds} = \frac{1}{D_2}\frac{dh}{d\alpha}$$

$$= \frac{1}{D_2}\frac{-32\beta^4\alpha H}{(1+16\beta^4\alpha^2)^2} \qquad (7)$$

And $$S = D_2\alpha \qquad (8)$$

2 - Correlation of Controlling Parameters H, D_1 and D_2 with M_s and Δs

The several differentiations of h with respect to α show that α varies inversely with β^2 or

$$\alpha = \frac{K}{\beta^2} \tag{9}$$

where K is a number > 0 and equal to $\frac{1}{4\sqrt{3}}$ for maximum magnification. Substituting equation (9) into equation (3) we have

$$M_\alpha = \frac{-32\beta^4 \frac{K}{\beta^2} H}{\left(1 + 16\beta^4 \cdot \frac{K}{\beta^4}\right)^2}$$

$$= \frac{-32 K \beta^2 H}{(1 + 16K^2)^2} \tag{10}$$

Since $M_s = \frac{dh}{d\alpha} \cdot \frac{d\alpha}{ds}$

And $\alpha = s/D_2$; $\frac{d\alpha}{ds} = 1/D_2$, Equation (10) becomes

$$M_s = \frac{-32 K D_2^2/D_1^2 \cdot H}{(1 + 16K^2)^2} \cdot \frac{1}{D_2}$$

$$= -\frac{32K}{(1 + 16K^2)^2}\left(\frac{D_2 H}{D_1^2}\right) \tag{11}$$

which indicates that for any given value of α, M_s increases with H β and D_2 and decreases with D_1 increasing.
Further, with $s = \alpha D_2$ from equations (8) and (9)

$$s = \frac{KD_2}{\beta^2} \tag{12}$$

which is equivalent to

$$s = \frac{KD_1^2}{D_2} \tag{13}$$

which shows that for any given value of α , s increases with D_1 and decreases with β and D_2. Similarly $\Delta s = \Delta\alpha \; D_2 = \frac{(\Delta K) D_1^2}{D_2}$ increases with D_1 and decreases with D_2 and β.

The deductions then from equations (11) and (13) assist in obtaining suitable values of M_s and Δs. Having chosen

D_1 and D_2 and H to obtain a desired M_s and Δs, M_s will then vary with s as equation (7) which can be rewritten:

$$\frac{dh}{ds} = \frac{-32\beta^4 \frac{H}{D_2} S}{\left(1+16\beta^4 \frac{S^2}{D_2^2}\right)^2} \cdot \frac{1}{D_2}$$

or
$$M_S = \frac{-2CHs}{(1+Cs^2)^2} \qquad (14)$$

where $C = 16 \frac{D_2^2}{D_1^4}$

Rewriting equation (9) $\alpha = 1/2\sqrt{3}\beta^2$

$= s/D_2$

$= D_1^2/2\sqrt{3}\, D_2^2$

And $S = \frac{D_1^2}{2\sqrt{3}\, D_2}$ for M_s (max) so that equation (14) is increasing for values of $s < \frac{D_1^2}{2\sqrt{3}\, D_2}$ and decreasing for values of $s > \frac{D_1^2}{2\sqrt{3}\, D_2}$

Since the deductions of equations (11) and (13) are opposing, it is evident that to obtain high magnifications we must sacrifice range Δs.

Summarizing, we have:

Increased M_s	Increased Δs
Increase H	Increase D_1
Increase D_2	Decrease D_2
Decrease D_1	Decrease β
Increase β	

The locus of the M_s maximum points on varying β and s is a rectangular hyperbola $M_s = \frac{-3/8\, H}{s}$

In any case, equation (3) indicates magnification can be increased by increasing H as M_α or M_s are directly proportional to H.

Confining H to low pressures so that compressibility effects will not impose further complications on theory, we find that for $\frac{\Delta P}{P_1}$ at each orifice to be not greater than .01:

$$\frac{h - 407.20}{h} = .01$$

and $h = 411.32$ inches water absolute (max.h)

Also for $\frac{H-h}{H} = .01$

$H = 415.50$ in. water absolute

$= 8.30$ inches H_2O gage

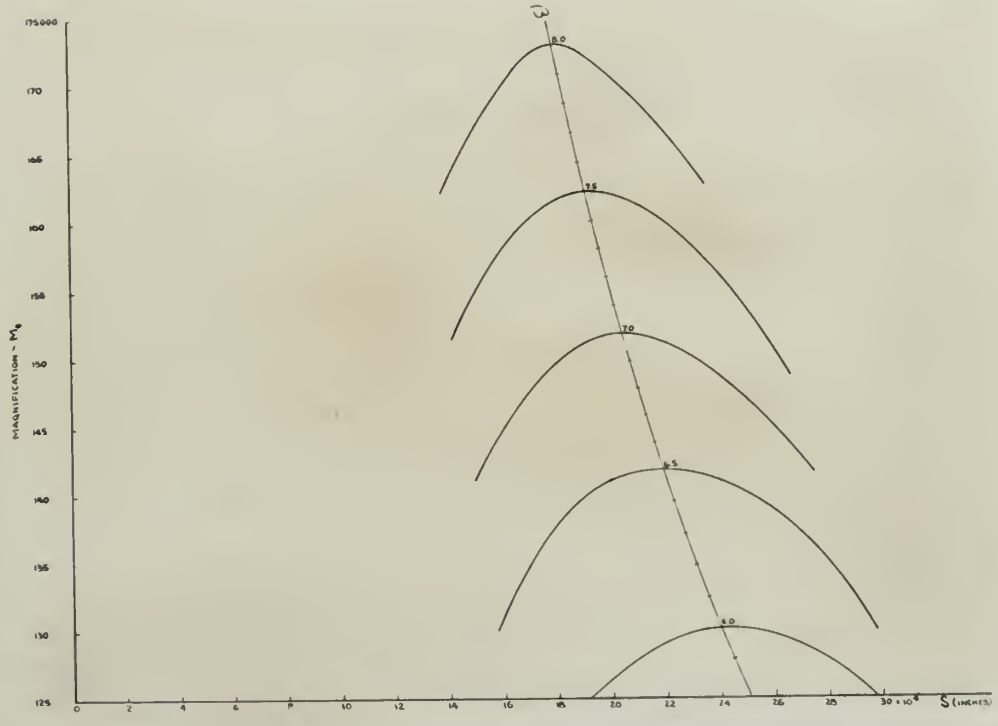

Figure 3a - Design curves

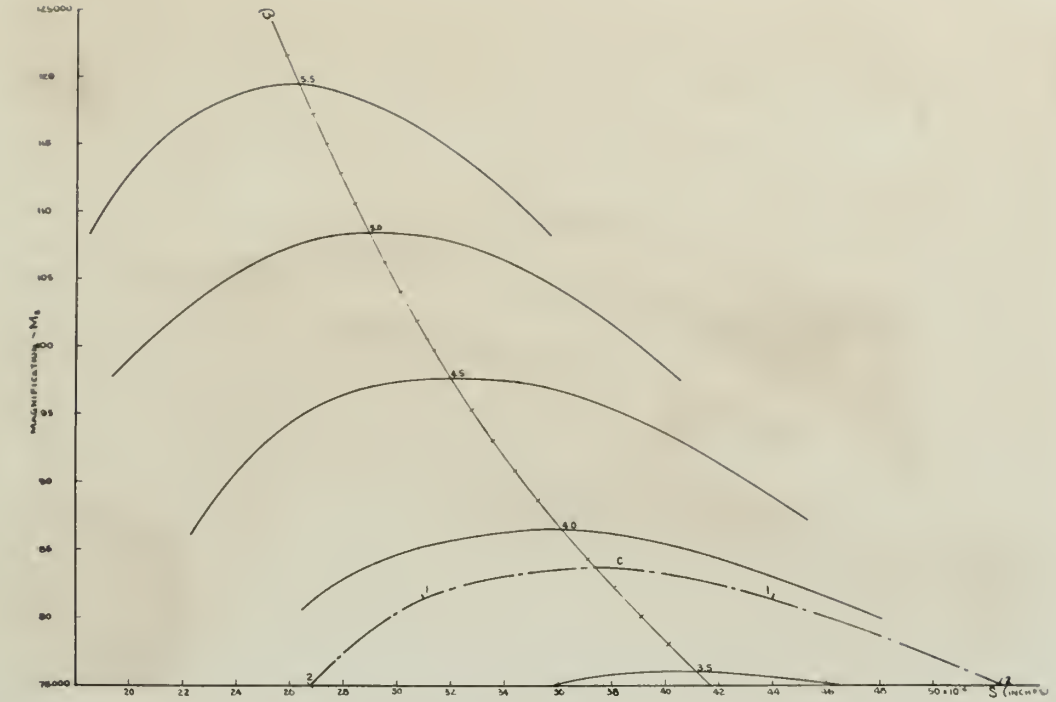

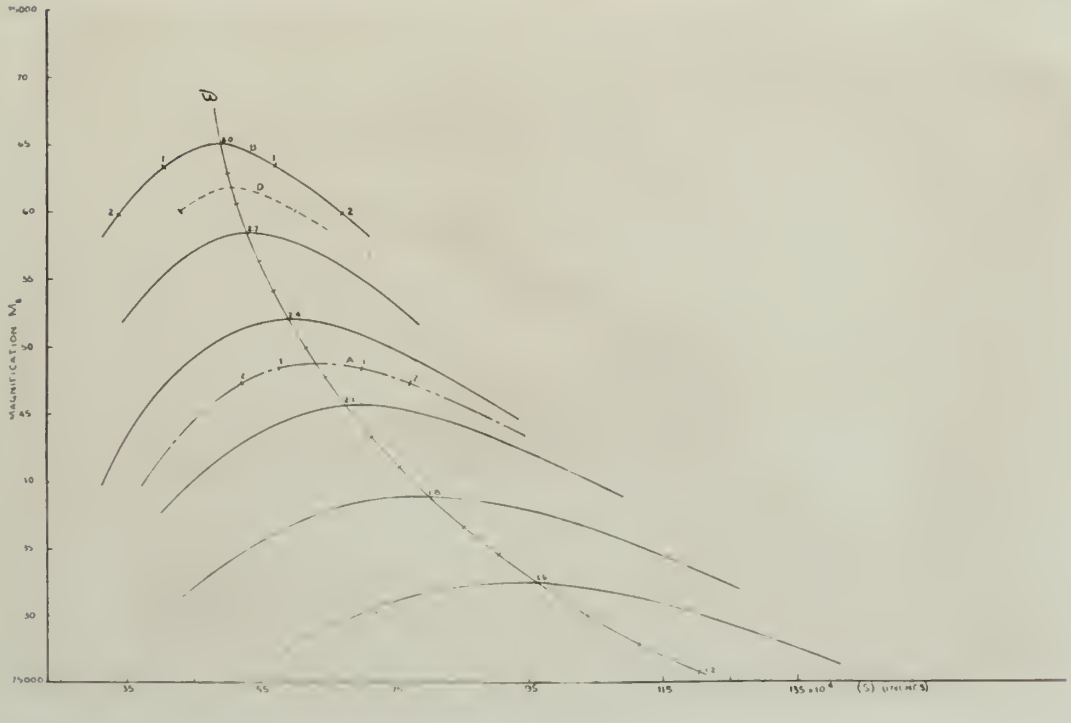

Figure 3 b and c - Design curves

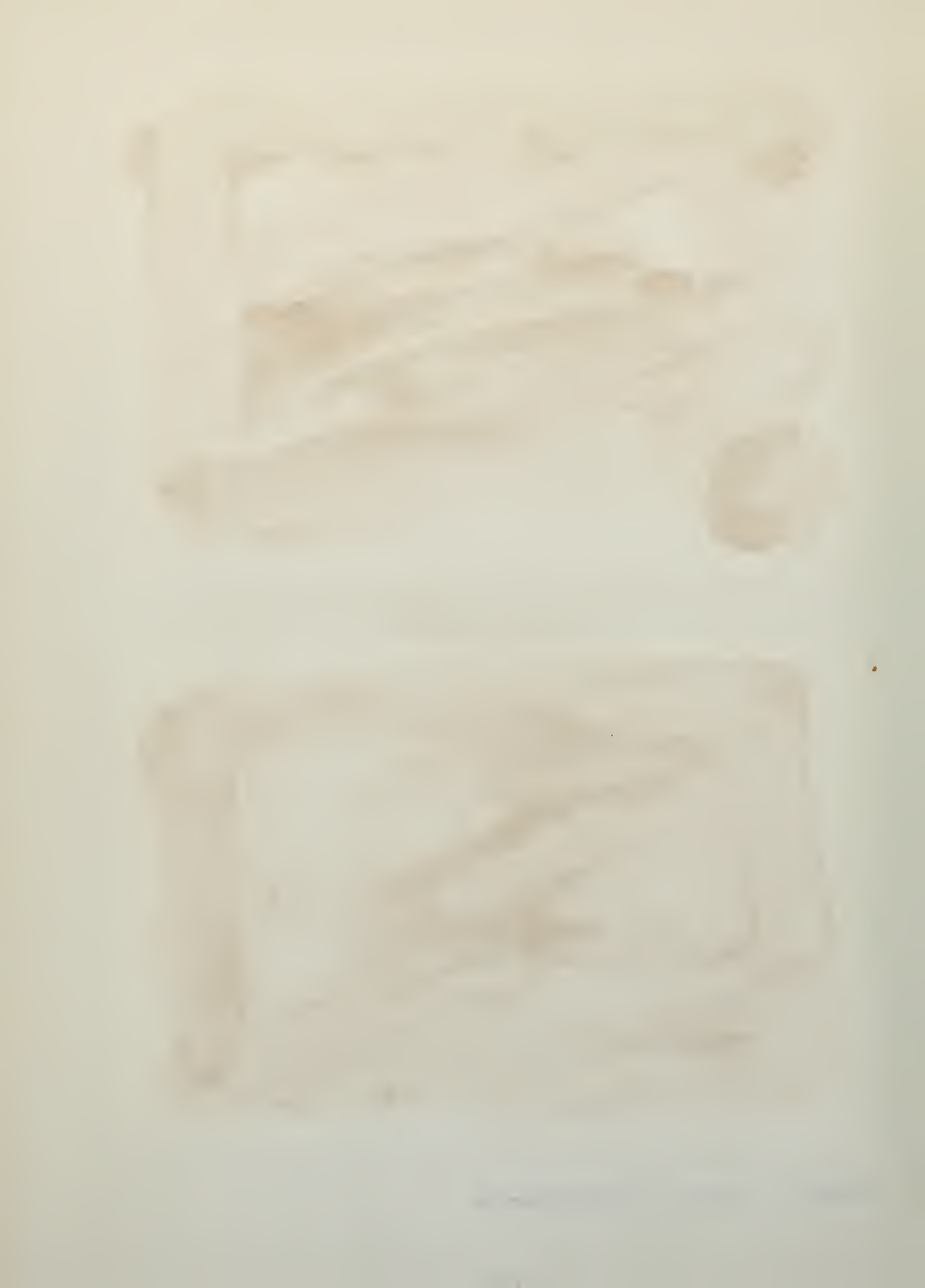

At this point it is desirable to summarize the foregoing information in the form of general $\underline{M}_s$ vs. $\underline{s}$ curves for various values of $\underline{\beta}$ which are determined from a knowledge of the practical limits to which a machinist can reproduce $\underline{D}_2$ and $\underline{D}_1$.

Since existing shop technique makes a .001" diameter hole well within the realm of practicability $\underline{D}_1$ (min) is taken at this value.

It can be seen that if $\underline{M}_s$ is plotted versus $\underline{s}$ for an arbitrary range of ($\underline{\beta}$ and $\underline{s}$) and for a $\underline{D}_1$ of .001", (see Figure 3 a,b,c on pages 9 and 10), that the curves can be extended for use with any $\underline{D}_2$, $\underline{D}_1$, $\underline{M}_s$ and $\underline{s}$ since from equation (7):

$$\frac{dh}{ds} = \frac{1}{D_2}\frac{dh}{d\alpha} = \frac{1}{\beta D_1}\frac{dh}{d\alpha}$$

or

$$\frac{dh}{d\alpha} = \beta D_1 \frac{dh}{ds}$$

$$= \beta \times .001 \times \frac{dh}{ds}_{(D_1=.001")} = \beta \times (n \times .001) \times \frac{dh}{ds}_{(D_1=n\times.001")}$$

and

$$\frac{dh}{ds}_{(D_1=n\times.001")} = \frac{1}{n}\frac{dh}{ds}_{(D_1=.001")} \qquad (15)$$

Similarly from equation (8):

$$s = \alpha D_2$$

$$= \alpha\beta D_1$$

or

$$\alpha = s/\beta D_1$$

$$= \frac{s_{(D_1=.001")}}{\beta \times .001} = \frac{s_{(D_1=n\times.001")}}{\beta \times (n \times .001")}$$

and

$$s_{(D_1=n\times.001")} = n\, s_{(D_1=.001")} \qquad (16)$$

and

$$\Delta s_{(D_1=n\times.001")} = n\,\Delta s_{(D_1=.001")} \qquad (16a)$$

Accordingly, Figures 3 a, b and c were plotted for values of β of 1.5 to β = 8.0. It appeared that magnifications obtainable for values of $D_1 > .001"$ and $\beta < 1.5$ would be too low for expected useage. Further, with a $\beta > 8$ the range of use would be too small.

3 - Range of Use

It is anticipated that wire up to .150" diameter and of material varying from a soft copper with an elastic limit (EL) of about 5000 psi, $E = 15.6 \times 10^6$ psi, $\mu = .333$ up to a heat treated medium C steel of about 70,000 psi elastic limit, $E = 30 \times 10^6$ psi, $\mu = .303$ will be used since these properties are representative of the general run of engineering materials.

Suitable values of $\underline{\Delta s}$ then will be determined, using the two extremes of materials chosen.

First, choosing steel of .150" diameter, we have

$$\sigma = \epsilon_L E$$

$$\epsilon_L = \frac{\sigma}{E} = \frac{70000}{30 \times 10^6} = 2.33 \times 10^{-3} \text{ in/in}$$

$$\epsilon_T = \mu \epsilon_L = .303 \times 2.33 \times 10^{-3} = .707 \times 10^{-3} \text{ in/in}$$

$$\delta_T = \epsilon_T D$$

$$= .707 \times 10^{-3} \times .150 = 1.06 \times 10^{-4} \text{ in.}$$

Or $\underline{\Delta s}$ (maximum) for a medium C steel for use up to 70,000 psi will be about 10^{-4} inches.

For .150" diameter copper,

$$\epsilon_L = \frac{5 \times 10^{-3}}{15.6 \times 10^6} = .320 \times 10^{-3} \text{ in/in.}$$

$$\epsilon_T = .333 \times .320 \times 10^{-3} = .1068 \text{ in/in}$$

$$\delta_T = .1068 \times 10^{-3} \times .150 = 1.6 \times 10^{-5} \text{ in.}$$

Or $\underline{\Delta s}$ (maximum) for copper for use with its E.L. will be about 1.5×10^{-5} inches.

In view of this rough appraisal, it might be desirable then to design the gage for a $\underline{\Delta s}$ of 10^{-4} inches. It is desirable to design for a sufficiently large $\underline{\Delta s}$ so that the full elastic range of the material may be investigated for one setting of the gage.

In order to use the gage for smaller increments of $\underline{\Delta s}$ then, it will be necessary that sufficient sensitivity be designed into the instrument.

4 - Sensitivity and Magnification

The manometer scale is graduated in centimeters with a vernier to read to .01 centimeter. Based on being able to read the vernier to .01 cm = .00394" and that the human factor prohibits adjusting the vernier to the water column meniscus any better than .01 inches, the sighting instrument's sensitivity, ω is estimated at .01 inches.

For a $\Delta s = 10^{-4}$ inches with reading s taken every 10^{-5} inches and estimating a sensitivity magnification or multiplication factor of f = 10, the magnification required is:

$$M_s = \frac{f\omega}{\Delta s} \quad \text{(increment)} = \frac{10 \times 10^{-2}}{10^{-5}} = 10{,}000$$

Therefore, the gage will be designed for general use wherein the minimum magnification will be 10,000 and the minimum range of use 10^{-4} inches.

5 - Prediction of Magnification, Range of Use and Gap Clearance from various Combinations of Orifice Diameters

A study of Figure 3 indicates that a M_s of 10,000 can be obtained using many values of D_1. Recall from equation (15) that $M_{s\,(D_1 = nx.001")} = \frac{1}{n} M_{s\,(D_1 = .001")}$. If a D_1 of .001" is used, the values of M_s read from the curves are the same as the ordinate scale plotted. The following values of D_1 are tabulated as an illustration of Figure 3 useage for desired magnifications of 10,000 and, say, 20,000.

D_1 and	M_s (appearing on Fig. 3)	Converts to	M_s (desired)
.003	30,000	1/3 x 30,000	10,000
.007	70,000	1/7 x 70,000	10,000
.002	40,000	1/2 x 40,000	20,000
.005	100,000	1/5 x 100,000	20,000

Similarly it follows by using equations (16) or (16a) or $s_{(D_1 = nx.001")} = ns_{(D_1 = .001")}$ and $\Delta s_{(D_1 = nx.001")} = n\,\Delta s_{(D_1 = .001")}$ that the s or Δs read from Figure 3 depends on the value of D_1 being used. If D_1 = .001", the values of s and Δs read directly from the abscissa appearing on Figure 3 are the correct ones. Again values of D_1 are tabulated with certain possible magnitudes of s or Δs that may be encountered in using the curves. These are then corrected as follows:

D_1 and	s or Δs (as read from Fig.3)	Converts to	s or Δs (corrected)
.003	20×10^{-6}	$3 \times 20 \times 10^{-6}$	60×10^{-6}
.007	20×10^{-6}	$7 \times 20 \times 10^{-6}$	140×10^{-6}
.005	30×10^{-6}	$5 \times 30 \times 10^{-6}$	150×10^{-6}

Since Figure 3 has been plotted for a supply pressure $\underline{H}$ of 8.30 inches of water gage, if some other pressure is used, note by equation (7), it is necessary then, in using Figure 3, to multiply values of $\underline{M}_s$ read from the curve by the multiplicity of the new pressure. That is, if an $\underline{H}$ of 10 inches were used, then $\underline{M}_s$ read from Figure 3 would have to be multiplied by $\frac{10.00}{8.30}$. Or with 5 inches $\underline{M}_s$ read must be multiplied by $\frac{5.00}{8.30}$.

Arbitrarily picking several $\underline{D}_1$ and $\underline{D}_2$ combinations that can be reasonably reproduced and that cover Figure 3 well, values of $\underline{M}_s$, $\underline{\Delta s}$, and $\underline{s}_1$ will now be estimated by using Figure 3.

$\underline{D}_1$	$\underline{D}_2$	$\underline{D}_2$ Drill Size	$\underline{\beta}$
.008	.0180	15	2.25
.006	.0180	15	3.00
.008	.0310	68	3.85

Taking the first combination, refer to Figure 3c and move to $\beta = 2.25$. There is no β curve plotted for this combination, so it is necessary to sketch one in with the aid of adjacent $\beta = 2.1$ and $\beta = 2.4$ curves already plotted. This appears as the dot and dash curve A .

Recalling that a $\underline{\Delta s}$ of 10^{-4} inches is desired for the gage, the range end points labeled ① are placed on the curve. This is accomplished by taking a strip of the same graph paper, laying off 10^{-4} inches on it, moving it up to Curve A and transferring the range end points. It is important to remember the points mentioned earlier in this section in laying off this strip to the correct $\underline{\Delta s}$. Since $\underline{D}_1 = .008"$,

then Δs to suit Figure 3 must be only 10^{-4} inches divided by 8 or 12.5×10^{-6}. This is a reverse process, using equation (16a), from that described earlier since we already have a desired Δs for a certain D_1 = .008" and have to make it suit the D_1 = .001" β-curve.

Now with Curve A plotted with its extremities defined, the magnification and s can be estimated. Reading the M_s scale for the end points ① of A, 48,200 is obtained. Again remembering equation (15), divide this M_s by 8 and 6000+ is obtained.

Extending the left end extremity ① of A down to the abscissa scale, 58×10^{-6} inches is read which when corrected as indicated by equation (16) gives 464×10^{-6} inches which is an estimate of the smallest gap opening s_1 on the gage during use. Of course s_2 will be $s_1 + \Delta s$, which in this case is 564×10^{-6} inches.

It will be observed that the magnification 6000 is less than that desired. Now, depending on the design of the strain gage, it may or may not already have some mechanical amplification built into it. If there is no mechanical advantage in the gage, then these values of M_s and Δs predicted by Figure 3 stand as is.

However, if for example, the gage is designed with, say a 2 to 1 mechanical magnification, that is, when the measuring follower of the gage moves 1/2 of the travel of the orifice tips, then there is still another consideration in using Figure 3.

In this case values of M_s read from Figure 3 should be

doubled and the Δs as covered by the actual gage will no longer be 10^{-4} but 2×10^{-4} inches. Then lay off on the abscissa strip 2×10^{-4} divided by 8 to give 25×10^{-6} which when transferred to curve A gives extremities labeled (2.)

Reading the ordinate from Figure 3, 47,300 is obtained which when divided by 8 gives 5900+ and when multiplied by the mechanical advantage of the gage results in a M_s of 11,800 which is within the requirements for total magnification.

Reviewing this process, without discussion, for the second combination of D_1 and D_2 tabulated on page 17 yields the following. This time assume there is no mechanical magnification built into the gage.

a. Sketch in $\beta = 3$ curve (in this case it is already plotted as a solid line)

b. Lay off Δs scale on strip of abscissa paper = $\frac{100 \times 10^{-6}}{6} = 16.6 \times 10^{-6}$ inches.

c. Transfer Δs to curve B.

d. Read ordinate of 63,000 from end points (1) of curve B.

e. Actual pneumatic magnification is 63,000/6 = 10,500.

f. Read abscissa of left end point of curve B as 40×10^{-6} inches.

g. Actual $s_1 = 6 \times 40 \times 10^{-6} = 240 \times 10^{-6}$ inches.

Once again, taking the third combination listed on page 17 and this time adding a mechanical advantage to the gage being used, the following procedure is obtained:

a. Sketch in $\beta = 3.85$ curve (appears as dot and dash curve C).

b. Lay off Δs scale on strip of abscissa paper = $\frac{200 \times 10^{-6}}{6} = 33.3 \times 10^{-6}$ inches.

c. Transfer to C by points (2)

d. Read ordinate of $M_s = 75,000$.

e. Actual pneumatic magnification is 75,000/8 = 9400-

f. Total magnification is 2 x 9400 = 18,800.

g. Read abscissa of left end point as 29×10^{-6} inches.

h. Actual $s_1 = 8 \times 29 \times 10^{-6} = 232 \times 10^{-6}$ inches.

The preceding discussion with examples covers a means of predicting magnification and gap clearance having available certain combinations of D_1 and D_2.

A more or less reverse procedure can be used when only magnification and Δs are known. Supposing a $M_s = 10,000$ and $\Delta s = 10^{-4}$ inches is desired as before. Suitable values of D_1 and D_2 can be predicted as follows:

A rbitrarily picking a $M_s = 60,000$ from Figure 3, it follows that D_1 must be .006" in order to give a M_s corrected of 1/6 x 60,000 = 10,000. With a $D_1 = .006$" then Δs to be used with Figure 3 is $10^{-4}/6 = 16.6 \times 10^{-6}$ inches. Transfer this to the 60,000 ordinate of Figure 3 c, so positioning it so that its end points lie favorably between the $\beta = 2.7$ and $\beta = 3.0$ curves. With the end points transferred to the figure, sketch in the β curve. Where it crosses the β line indicates a magnitude of 2.85 for β (in this case it is curve D).

Since $\beta = D_2/D_1$ then $D_2 = 2.85 \times .006 = .0171$ inches. Reading the left end point abscissa, s_1 is 43 x 10^{-6} inches corrected to $6 \times 43 \times 10^{-6}$ inches = 258×10^{-6} inches. Of

course with a mechanical advantage of n, the total magnification would be 10,000 n.

Table I and II below summarize the findings described in the foregoing.

TABLE I (Using only Pneumatic amplification)

Curve	D_1	D_2	β	$S_1 \times 10^{-6}$	Δs	M_s (Min)
B	.006	.0180	3.00	240	10^{-4}	10,500
C	.008	.0310	3.85	248	10^{-4}	10,200
D	.006	.0171	2.85	258	10^{-4}	10,000

TABLE II (Using both Pneumatic and Mechanical Amplification)

Curve	D_1	D_2	β	$S_1 \times 10^{-6}$	Δs (actual)	M_s (total)
A	.008	.0180	2.25	408	10^{-4}	11,800
B	.006	.0180	3.00	204	10^{-4}	20,000
C	.008	.0310	3.85	216	10^{-4}	18,800

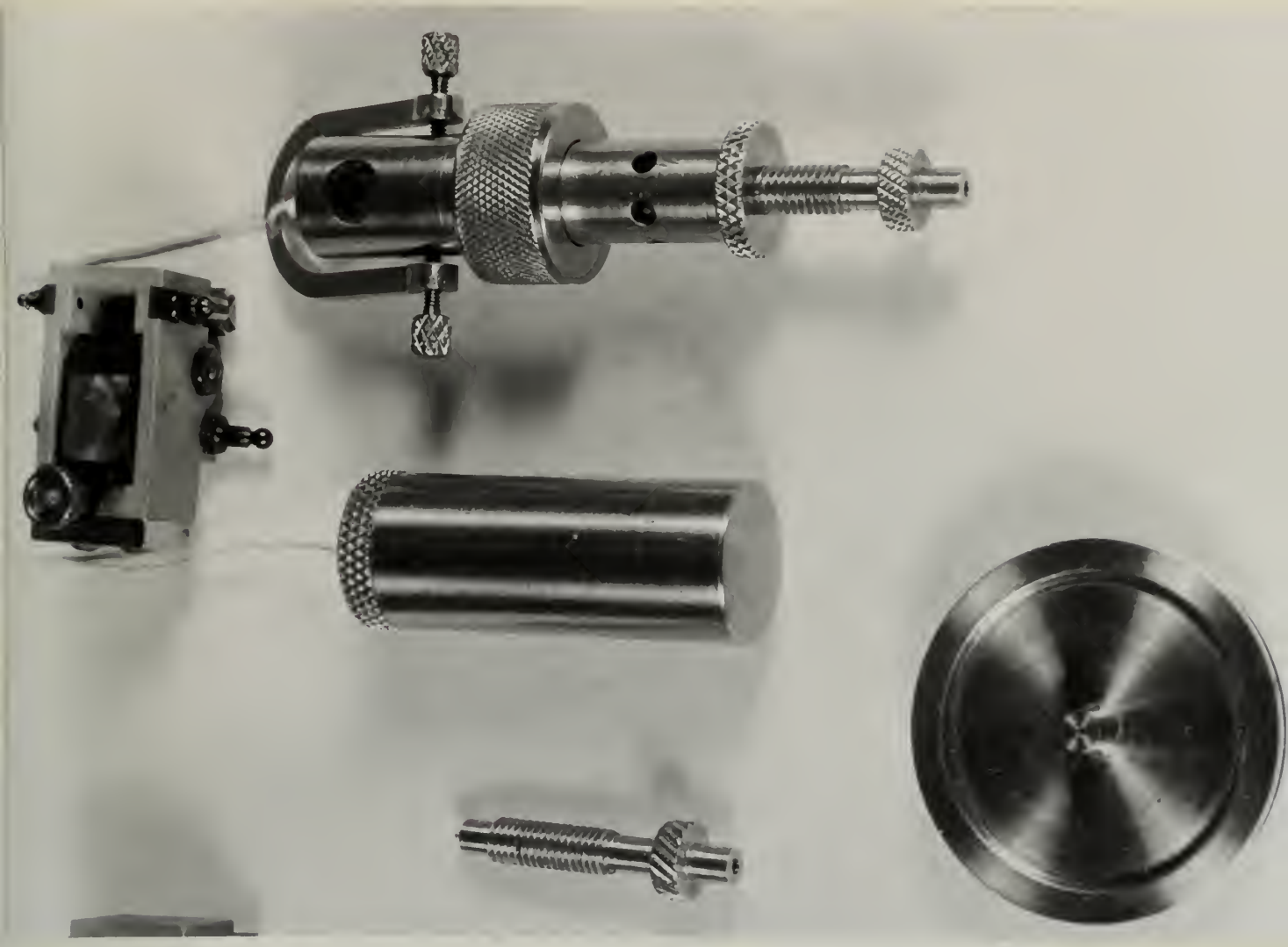

Figure 5 - Piston-type strain gage

Piston-type Strain Gage

Figure 4 (see Appendix) is a working drawing of a strain gage designed for use with wire up to .150" diameter. Figure 6 (see next page) is a diagram showing the gage in its working position. The wire under test is oriented in a horizontal direction, and passes between Piece 7 and 8 of the gage. Piece 8 is the piston follower which will move upward toward

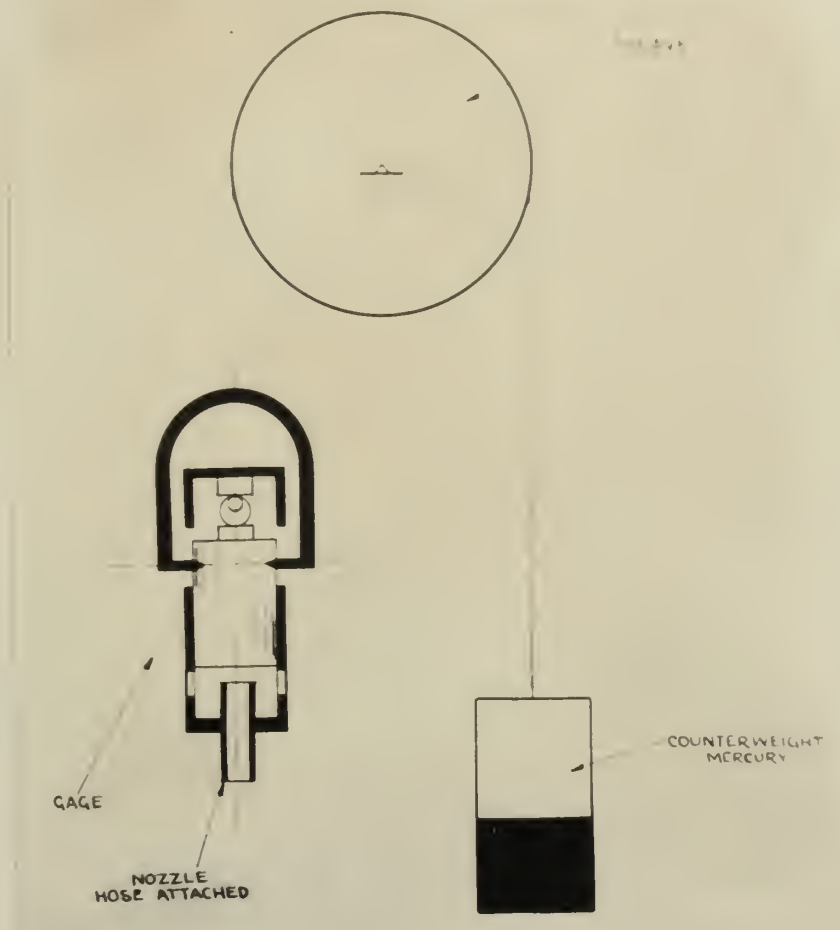

Figure 6 - Piston-type strain gage balancing arrangement

Piece 7 as the wire's diameter decreases in tension. As the follower rises, its lower end increases the gap between itself and Piece 4a, the orifice tip, which results in a Δs over that of the orifice tip's initial setting s_1. The other end of the nozzle is connected to a rubber hose which transmits the gas from the "Solex".

Of interest may be the weightless feature of the gage which eliminates any possibility of introducing a vertical sag component or bending in the small wire. Referring to

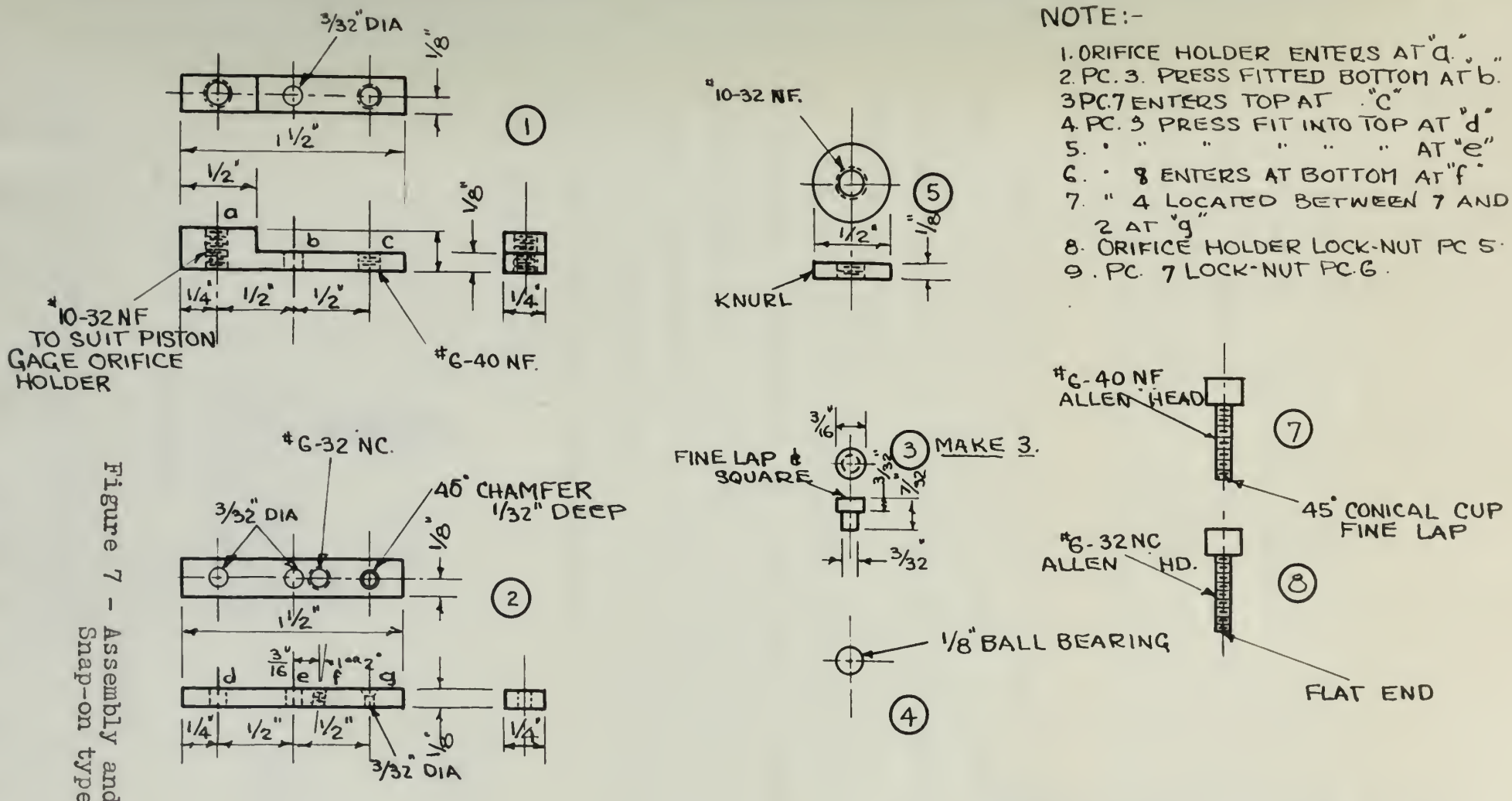

Figure 7 - Assembly and details of Snap-on type strain gage.

Figure 6, it will be seen that the upper end of the piston follower is connected to a yoke Piece 10 and thence by a cord over the sheave to Piece 16 which is a mercury weighted counterbalance. Thus, the weight of the gage and counterbalance is carried by the sheave pedestal. At the same time the piston cylinder assembly is free to fall about the piston by its own weight, which gives the contact pressure on the wire.

Another advantage of this arrangement is that unpredictable spring contact pressure, which is a working feature of other gages in use, is eliminated, and a positive constant pressure is insured.

The reliability of the gage, of course, is a function of the skill exercised by the machinist in adhering to the design dimensions. An imperfect bottom surface of the piston, a sloppy fit of the piston, friction in the moving parts or a rough tip surface, are all very critical items that will effect the gage performance.

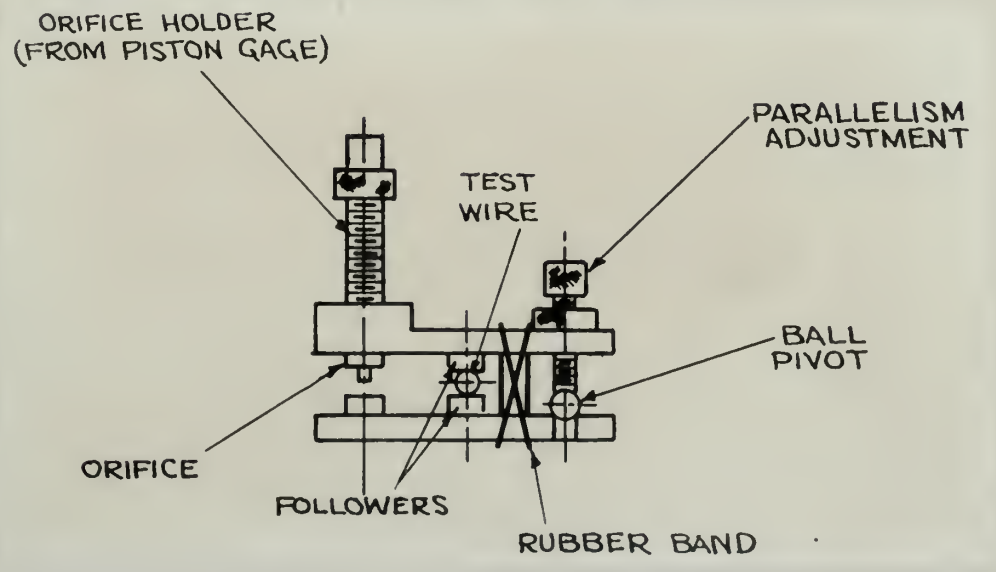

Figure 8 - Schematic of snap-on gage.

Snap-on Gage

The snap-on gage appears as Figures 7 and 8. It most pronounced features are its simplicity and ease of manufacture. The only actual fit between moving parts is at the ball pivot. Perhaps its greatest advantage is a built-in mechanical advantage, of two-to-one, which permits obtaining greater magnifications than can be obtained with the piston-type gage.

In operation, use is made of the orifice holder designed for the piston-type gage which is rather cumbersome and, if designed specifically for this gage, it would have been made much shorter. A rubber-band encircles both upper and lower plates to maintain contact with the wire being measured.

It is initially set in parallel by first inserting a sample wire, of diameter equal to that of the wire being tested, between the followers. Then the parallelism screw is adjusted until special feelers or inside calipers indicate both plates are parallel. The locknut on the adjusting screw is tightened simultaneously.

In order to prevent damage to the orifice when it is inserted, a stop screw (not shown on schematic) Piece 8, Figure 7, is provided which is always turned up against upper plate before removing gage from test wire. If this screw is not in position when gage is removed, the orifice will snap down and hit the orifice stop on the lower plate. Following the paralleling adjustment, the gage is calibrated as will be described later.

It should be noted that the action of the tip in this gage is the reverse of the piston type. That is, as the diameter of the wire being measured by this gage decreases, the gap clearance gets smaller instead of larger, as occurs with the piston-type. Consequently, initial orifice settings with the snap-on gage are designated as $\underline{h}_2$ or $\underline{s}_2$ instead of $\underline{h}_1$ or $\underline{s}_1$.

Tension Producer

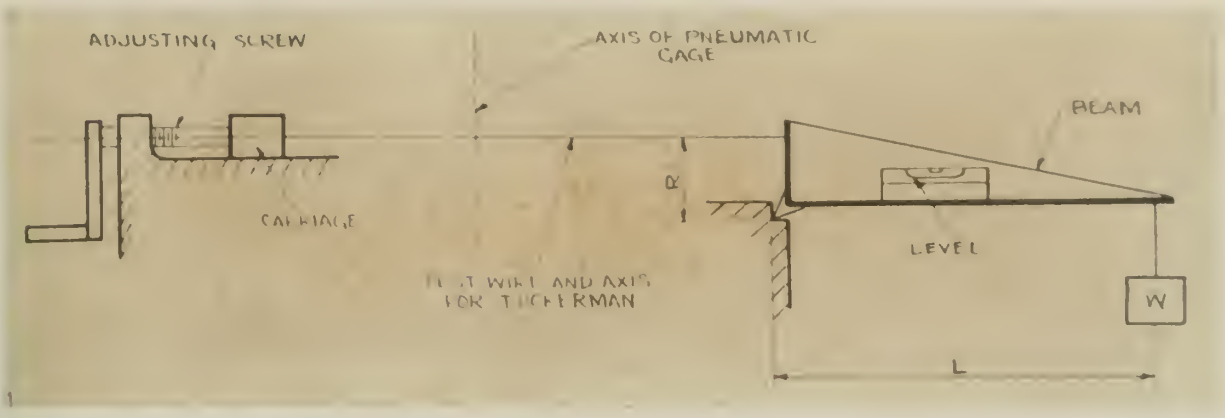

Figure 9 - Schematic of Tension Producer

The principle of operation of the tension producer is illustrated in Figure 9. Assembly and details of the producer appear as Figure 10 in the Appendix. This particular piece of equipment is designed to give tension to the wire in a horizontal plane to suit the weightless feature of the strain gage.

It has a mechanical advantage of 20 to 1 which is brought about by a simple lever arm reduction. Provision is made for leveling the beam lever arm initially and following each loading by moving the carriage by a lead screw. The ends of the wire are initially placed in the same horizontal plane by adjustment of jacking screws fitted to the beam support foundation.

The beam rotates on frictionless knife edge bearings. Loading is accomplished by adding weighed increments of lead shot to the bucket.

Lead shot is used so as to permit loading of the wire without impact, simply by pouring the load.

The tension producer beams are designed so that at maximum loading the deflection of the beam will be negligible so far as the deflection's shortening effect on the lever arm is concerned. With a bucket loading of 62.5 pounds, the stress produced in a .150 inch wire will be 70,000 pounds per square inch.

Interferometer

Figure 11 is a schematic showing the working elements of the interferometer used to calibrate the strain gages. It was designed primarily for other use, but by addition of an adaptor and setting it on end, it was made suitable for calibration.

Essentially, it consists of a foundation (shown vertically) to which is mounted, by elastic hinges, a movable table. The table is raised and lowered against its own weight by the micrometer screw actuated by a hand wheel. Moving with the table is the lower of two optical flats which when raised approaches the other optical flat suspended on a fixed pedestal by three differential adjusting screws. A microscope with adjustable cross-hairs is mounted above in a position to view the interference fringes produced. A mercury arc light is located below the flats together with a filter.

The adaptor consists of the yoke and sheave which normally supports the piston-type gage together with two calibrating pins A and B. The pins are of smaller diameter

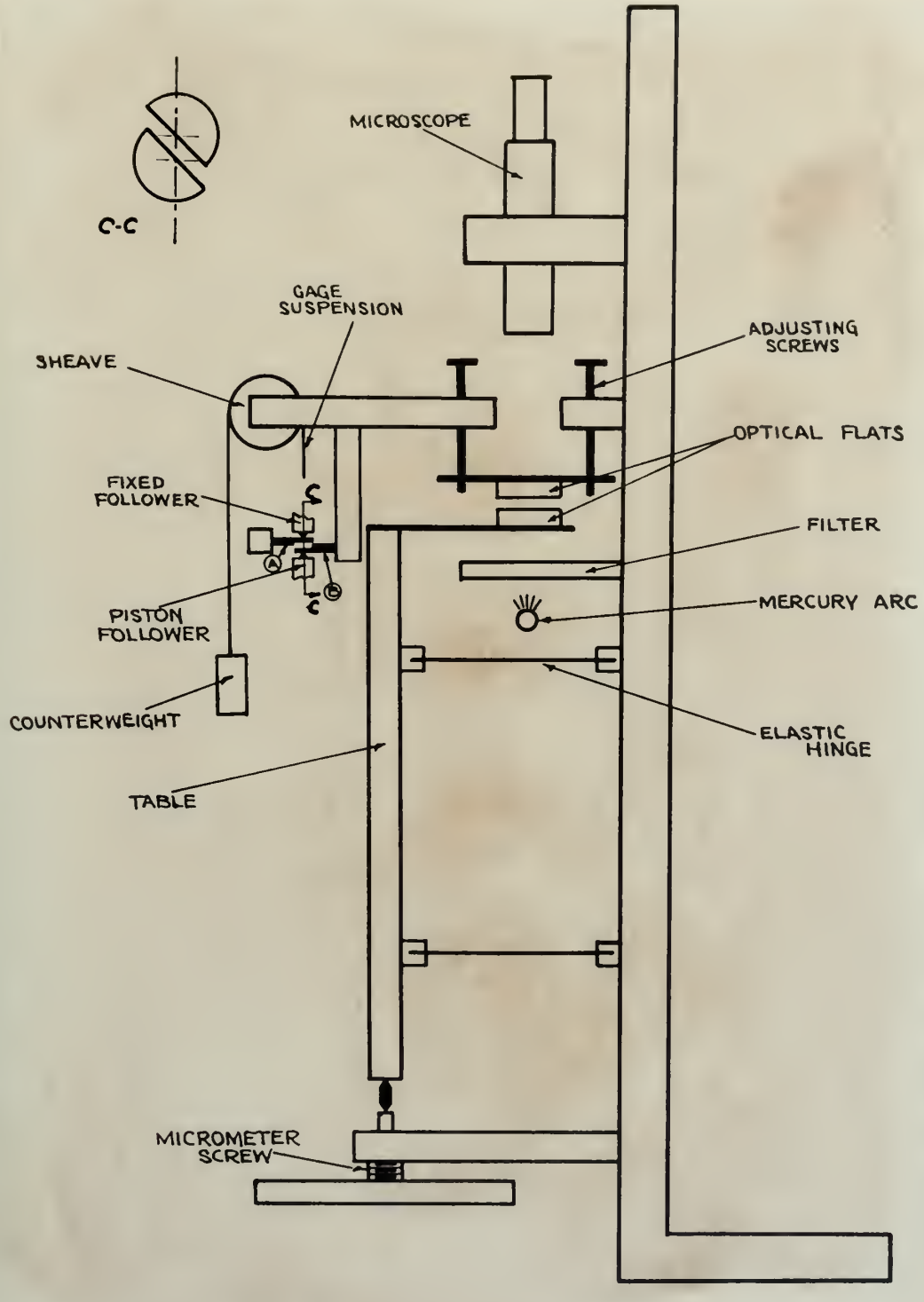

Figure 11 - Schematic of Interferometer

than the wire to be tested and are machined so that their ends overlap. (Note section C-C of Figure 11) By this provision, the pins can be made to line up with each other and to separate so as to effectively increase their diameter. Pin A is attached to a frame which is mounted to the interferometer table. Pin B is attached to a rod which in turn is connected to the fixed pedestal of the interferometer. By turning the interferometer screw so as to raise the table, pin A moves upward and away from pin B.

It can be seen that if a strain gage is attached across the pins, the gage followers will move with the same action as occurs when the diameter of a test wire is caused to change.

In use, with a gage suspended on the pins, the micrometer screw is adjusted so as to make the effective diameter across the pins equal to the test wire. Then the optical flats are brought together so as to produce Newton's fringes of a fairly good spacing and the microscope cross-hairs lined up on a fringe boundary. With the orifice of the gage brought into the correct spacing as indicated by the "Solex" manometer reading, calibration is begun by backing off on the micrometer screw so as to pass one fringe at a time across the cross hairs of the microscope. This means then, that the pins A and B have come closer by one-half a wave length of mercury light.

1 - Piston-type Gage

Calibration with this gage proved unsuccessful. Sensitivity and good magnification was achieved but reliability was lacking. At times fairly consistent runs, over a Δs of 10^{-4} inches using the several orifice combinations listed in Table I, could be gotten, but they could not be repeated. After taking several corrective measures and observing the results attained, it was decided that the main difficulty was inferior workmanship. Among the corrective measures taken were: -

1. Taking apart gage, removing piston and carefully facing off and lapping end of piston to which orifice is directed. The original face was very rough and showed tool marks clearly.

2. Refinishing follower pieces which were not straight.

3. Recentering fixed follower which was off-center with moving follower.

4. Adding weights to both gage and counterweight to insure good contact on the wire.

5. Thorough cleaning of gage and lubrication with light oil.

Inspection of the gage disclosed the following remaining defects which could not be corrected in sufficient time to permit completion of calibration and test.

1. Cylinder walls stepped so that piston was tighter at one end than the other.

2. Perceptible shake of upper end of piston when in cylinder.

3. High spots on piston.

4. Poorly fitting keys at top of piston.

5. Orifice holder thread engagement with cylinder bottom sloppy.

6. Dimensions not closely adhered to.

Inasmuch as good results intermittently appeared when using this gage, it is believed that with good workmanship, a gage of this type could be used satisfactorily. A little further attention to the existing ga ge might also be well worthwhile.

2 - Snap-on Type Gage

Since efficient operation of the piston-type gage was found to rely so greatly on the quality of fits of moving parts, it seemed worthwhile to consider some other alternative that did not have these characteristics. Consequently, the snap-on type (described earlier) was devised and was found to give good results.

The orifices used were those combinations appearing in Table II page 21 and the supply pressure H was 8.30 inches of water. The calibration and test procedure follows:

a. Weigh out lead shot at suitable load increments to cover stress range desired in test wire and place in convenient containers ready for loading tension producer.

b. Set up tension producer with test wire in place and give it an initial load so as to insure knife-edges seating properly, that wire is straight and all play is taken out of entire arrangement. Using a surface gage on foundation of tension producer together with a dial indicator, level test wire by adjusting jacking screws located at base of beam mounting pedestal. Level beam by adjustment of carriage lead screw with special socket ratchet wrench provided until spirit level on beam indicates beam is level.

c. Mount Tuckerman strain gages on each side of wire so that any slight bending occurring during loading will be taken care of by averaging Tuckerman readings. Set up collimators and adjust gages so as to permit centering collimator light image in collimater field. The Tuckerman gages are suspended as shown in Figure 13b by a cord and a linkage holding upper.

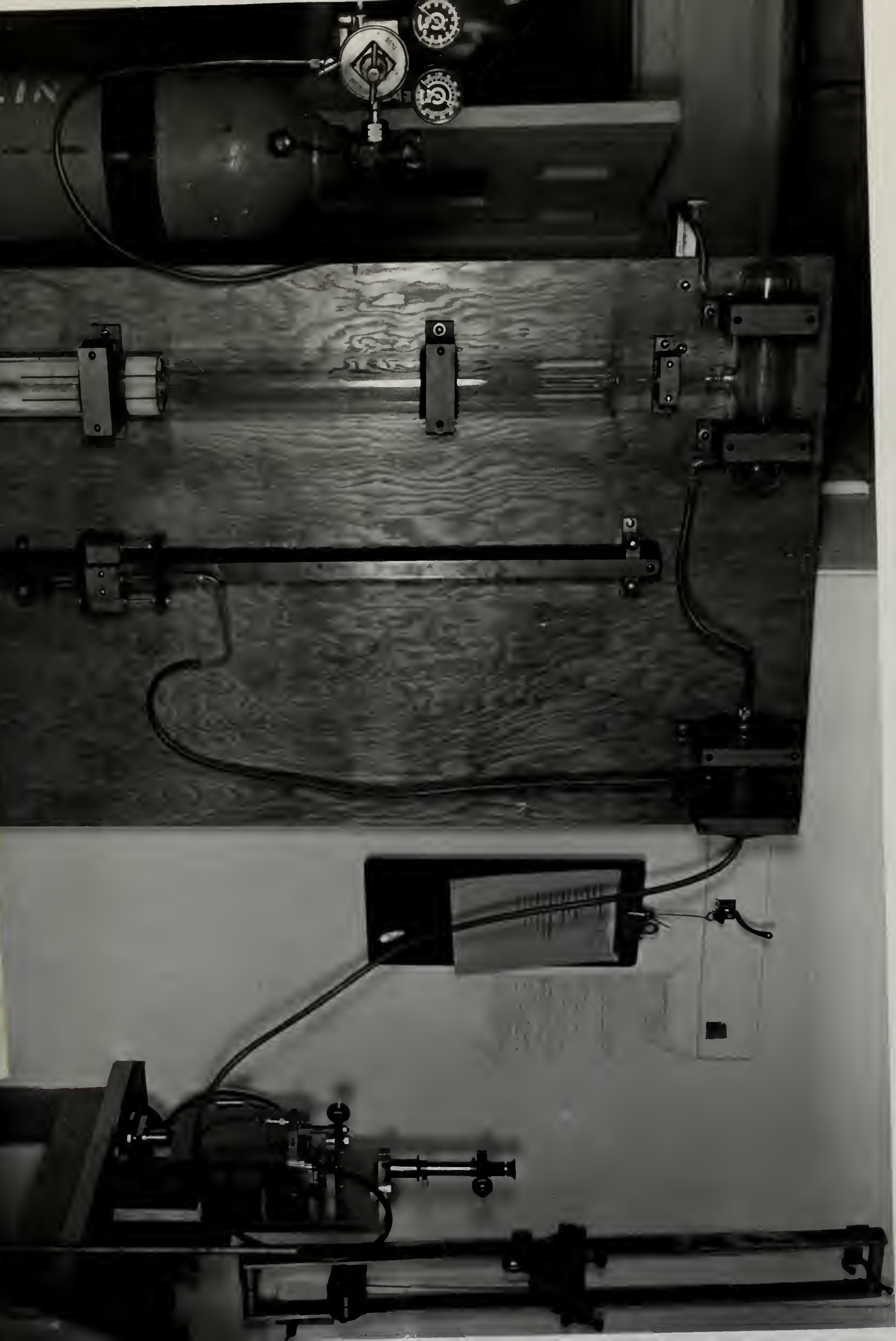

... of calibration

side mounting pins together. The lower side is held together by a rubber band secured over lower mounting pins.

d. Level "Solex" mounting by base adjusting screws until level, as indicated by spirit level. Place primary orifice D_1 in left end of intermediate chamber and reconnect hose connection. Check the "Solex" for H = .3 psig and for leaks. This is done by admitting the air or nitrogen to the plunger (refer to Figure 1) until the gas bubbles out the bottom at a slow rate. (about 1 bubble every 5 seconds is satisfactory) If the rate is much faster, the meniscus in the manometric column will not settle down. Making sure the outlet from the intermediate chamber is open, read the bottom of the meniscus in the column. This is h_o. Then squeeze the hose connection leading from the intermediate chamber until the meniscus stops falling. If the meniscus does not recede to the point opposite the bottom of the plunger, the system is leaking. When the system is tight, read the meniscus which will be h_c. H then is equivalent to $h_o - h_c$. If $h_o - h_c$ is greater or less than H and the system is tight, drain off or add water to the tank until H is at desired value.

e. Turn on interferometer light source and with adjusting screws on upper flat, bring flats close together until fringes are about 1/8" apart as appears to the eye. The fineness of the bright lines can be adjusted by wrapping the light source with tin foil with a pin point hole pressed through the foil on the side that light is desired. The smaller the aperture, the finer will be the bright lines, the smaller the field of fringes and the less the light intensity.

The calibration pins A and B are set to the diameter of the test wire by micrometers in the vertical direction. In the horizontal direction they are set to the diameter of the pin so that when closing the pins together by micrometer screw, they will ultimately close to an effectively solid wire of diameter equal to their individual pin diameter.

f. Place snap-on gage on test wire, insert orifice to be used and connect "Solex" hose. Center gage followers by eye and then turn in orifice so as to close gap clearance until "Solex" manometer water level reads about 1/2H. h_o is known so that h_2 now will read h_o - 1/2H or h_c + 1/2H. Center gage exactly by use of inside calipers or special feeler piece set by micrometers. The calipers are set to a spacing of .500" (distance between follower centers and orifice center) minus the sum of the test wire radius plus the orifice holder tip radius. Recheck h_2 so that it still registers at the 1/2 H point.

g. When gage is centered properly and h_2 on manometer reads correctly, remove gage (first turning in protective stop screw) and place on calibrating pins. Recenter gage. This time the calipers are set at .500" - (radius orifice holder tip + radius of calibrating pins). Leave gage at this point and adjust interferometer screw until h_2 reads as before at h_o - 1/2 H. Conditions are now such as to permit calibration and the gage is set at the exact diameter of the preloaded test wire.

h. The cross-hair of microscope is brought to the sharply defined edge of a bright fringe by the cross-hair

adjusting screw. The calibration run is now begun by carefully slacking off micrometer screw so as to pass one bright fringe across cross-hair at a time. After each setting the water column is read and recorded. Table IV of Appendix lists data taken for the three combinations of orifice sizes used. The run continues until the water column reading passes well through the reading corresponding to 3/4H which the theory shows is the point of maximum magnification. Review of the readings taken on this run shows whether sufficient Δs or range has been covered. The number of readings taken multiplied by one-half the wave length of mercury light (10.75×10^{-6} inches) gives the Δs covered. If in this case it is over 10^{-4} inches, it is advisable to space the readings on each side of the 3/4H point by inspection so as to give $\Delta s = 10^{-4}$ inches, pick from data taken a new starting point, and then reset the gage as before to give the suitable h_2 or initial reading. This means resetting the gage on test wire, getting desired h_2, moving back to calibrator and making final calibration runs.

Four calibration runs were made for each combination of orifices.

i. After calibrating, the tension producer is checked again for initial position for starting test run.

j. The gage is now removed from the calibration device and recentered on test wire. This time, however, the orifice adjustment is left untouched and h_2 should check its original reading. If it is close to reading correctly, a

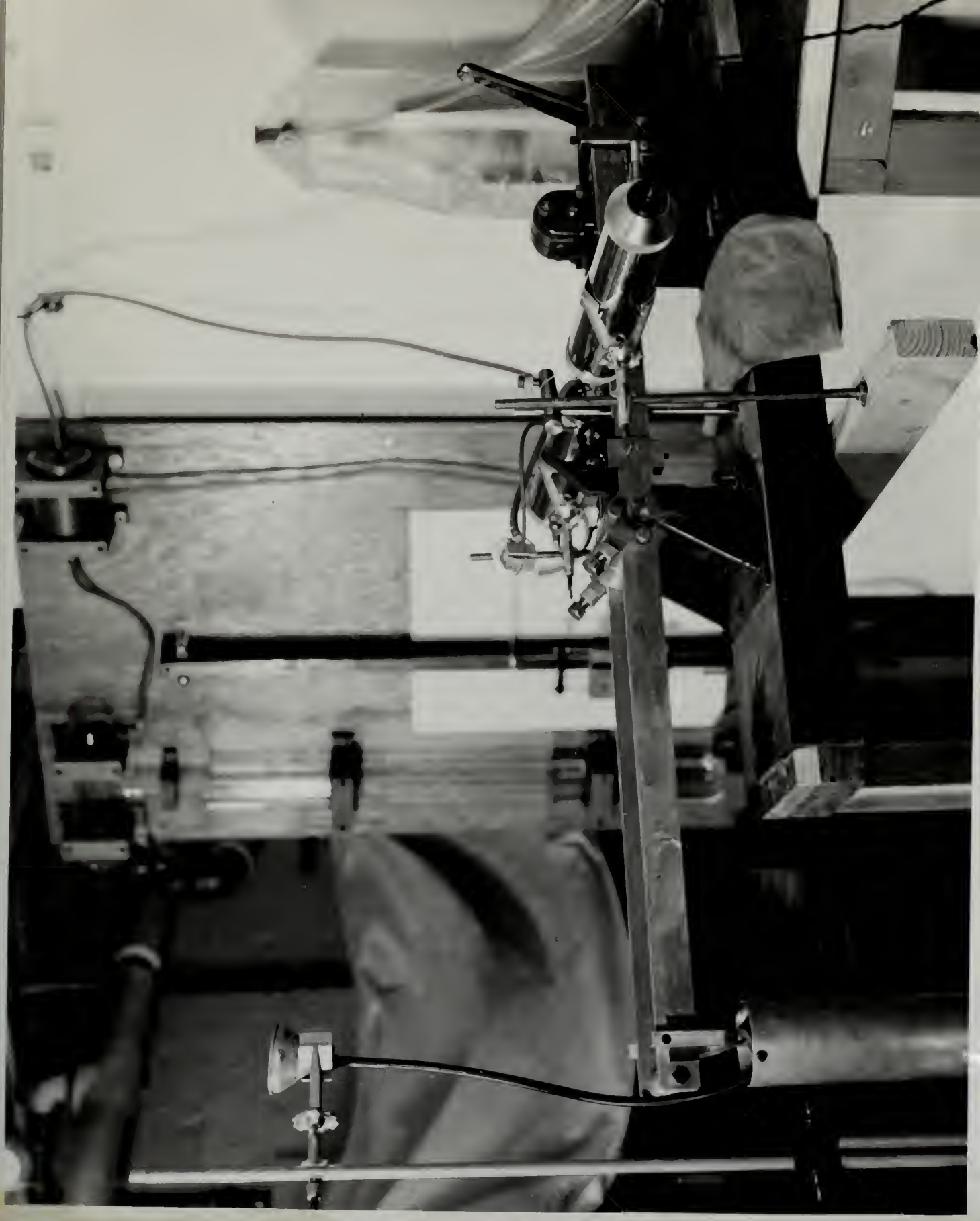

Figure 13a - Photograph of actual run (snap-on pneumatic gage, Tuckerman, tension producer, "Solex".)

Figure 13b - Photograph showing Tuckerman and strain gage arrangement on wire.

very slight pressure by the finger will move it in without changing center position. If it is far off, the gage should be recalibrated.

k. When h_2 repeats itself on the test wire, the test run is begun. Take initial readings of h and read both Tuckerman strain gages. With funnel arrangement shown in Figure 13a, pour in load increment into bucket and turn carriage lead screw until beam is level as indicated by spirit level. Take Tuckerman and manometer readings after each loading and leveling until desired loading range is covered. Table V is a compilation of the test data taken using the snap-on gage.

3 - Reduction of Data and Curves Plotted

Expansion by division of equation (1) indicates that in the section of the curve used, that is near the point of maximum magnification, which is located in the region to the left in Figure 2a, that the function can be closely approximated by a parabola. Further to the right it approaches a straight line.

With this in mind the data of Table IV was grouped and tabulated so as to give parabolic and straight line equations for purposes of plotting. Table VI Appendix lists the suitable equations developed for plotting the calibration curves. The equation parabolic or straight line which most nearly suited the data taken is underlined.

From Table V, Table VII was computed for plotting Figure 15 and determining the value of Poisson's Ratio for the wire. Since within the elastic range of a material, it is expected that strain relations remain linea r, a straight line equation was found suitable to the data taken. These equations used in plotting Figure 15 also appear in Table VI in the Appendix.

Table VII was obtained by:-

a. Correcting the Tuckerman readings by their characteristic correction factors.

b. Averaging the corrected readings.

c. Tabulating their summations from a zero reference to give ϵ_L.

d. Correcting h read from manometer in centimeters to inches from a zero reference.

e. Converting h to s or δ_T by reading calibration curves, Figure 14.

f. Dividing values of δ_T by wire diameter to give ϵ_T

From the values of δ_T tabulated in Table VII Figure 16 was plotted to show the reliability inherent in the arrangement while using three independent orifice combinations.

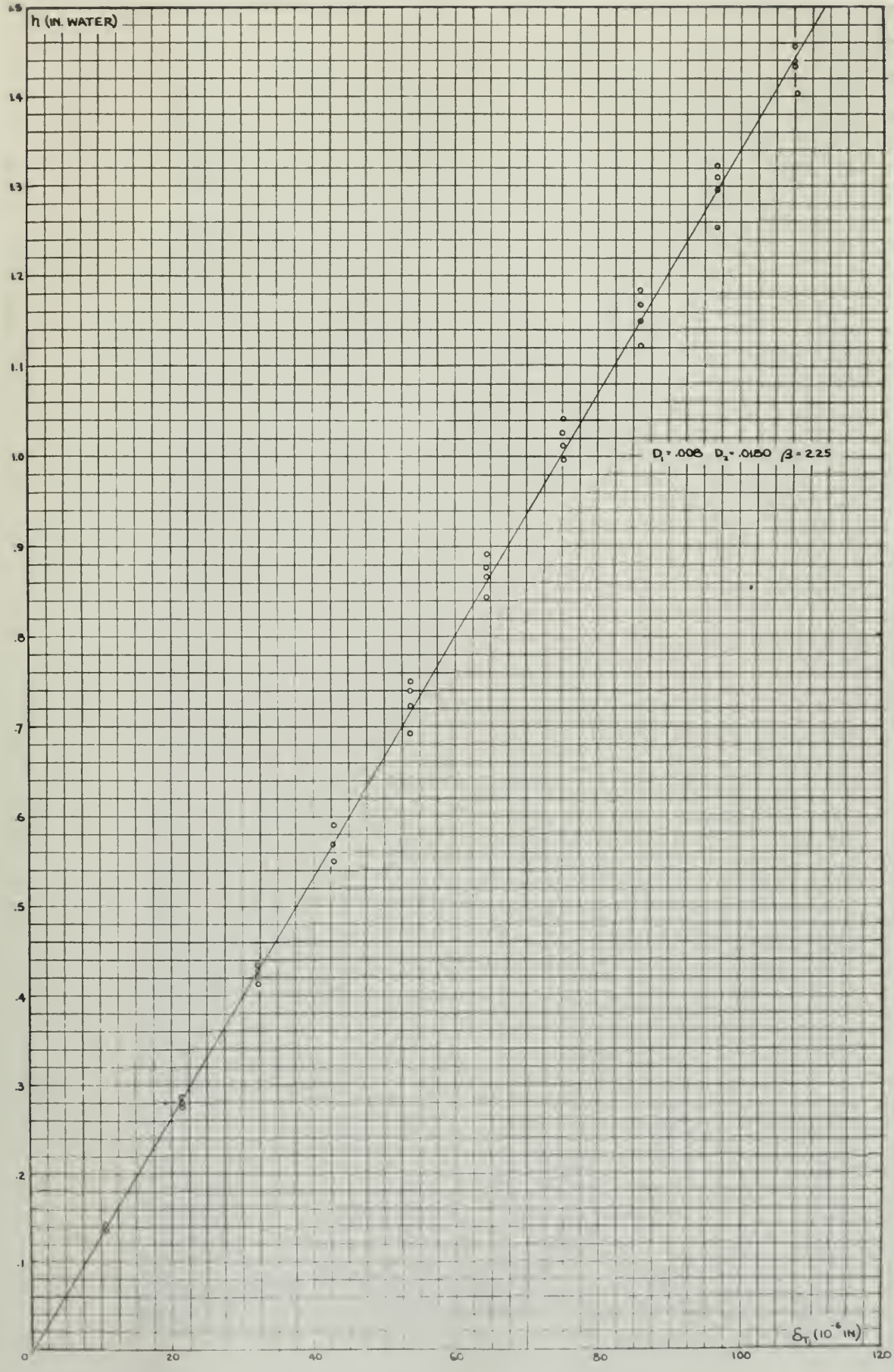

Figure 14a - Calibration curve, Combination A.

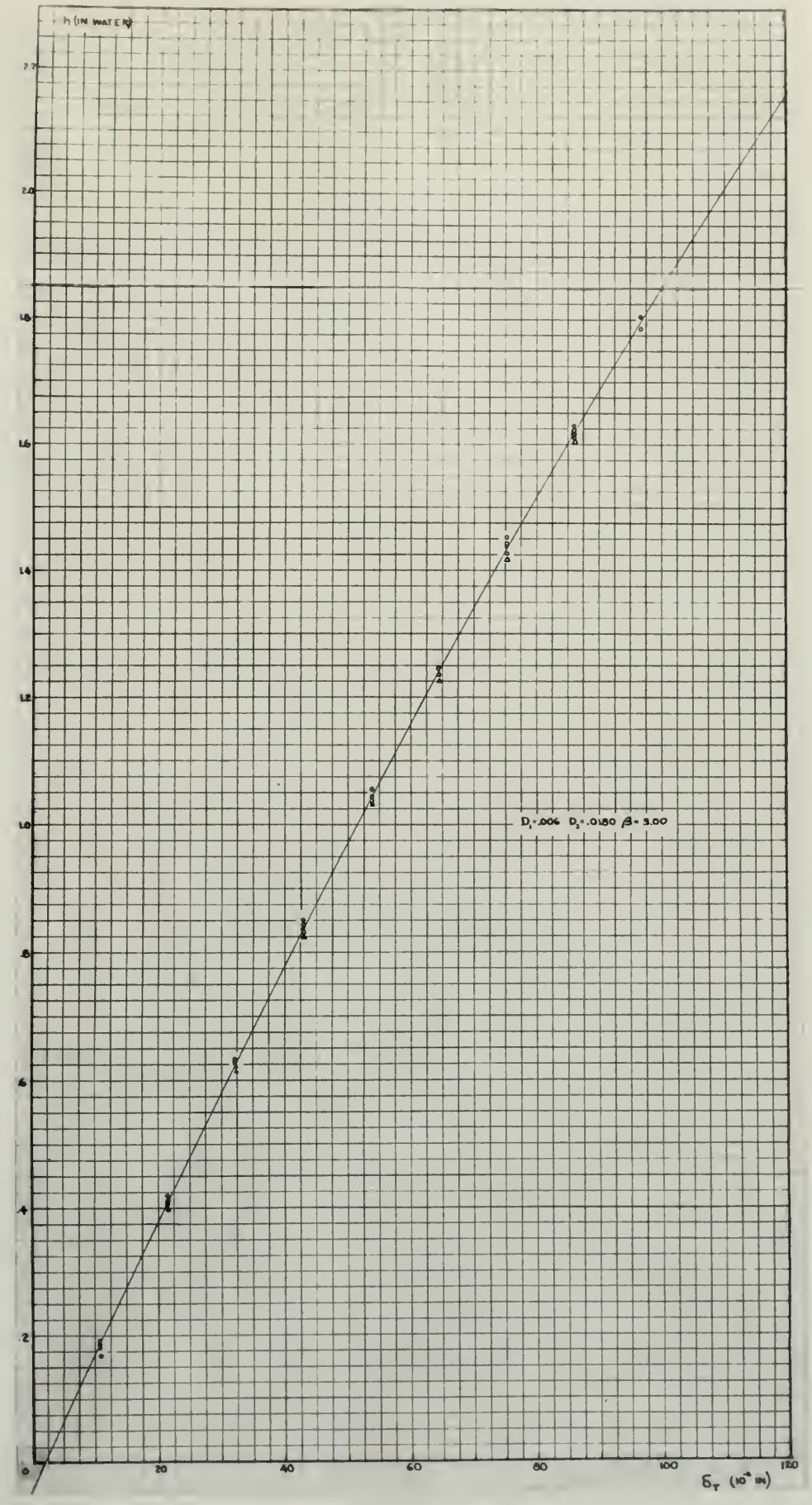

Figure 14b - Calibration curve, Combination B.

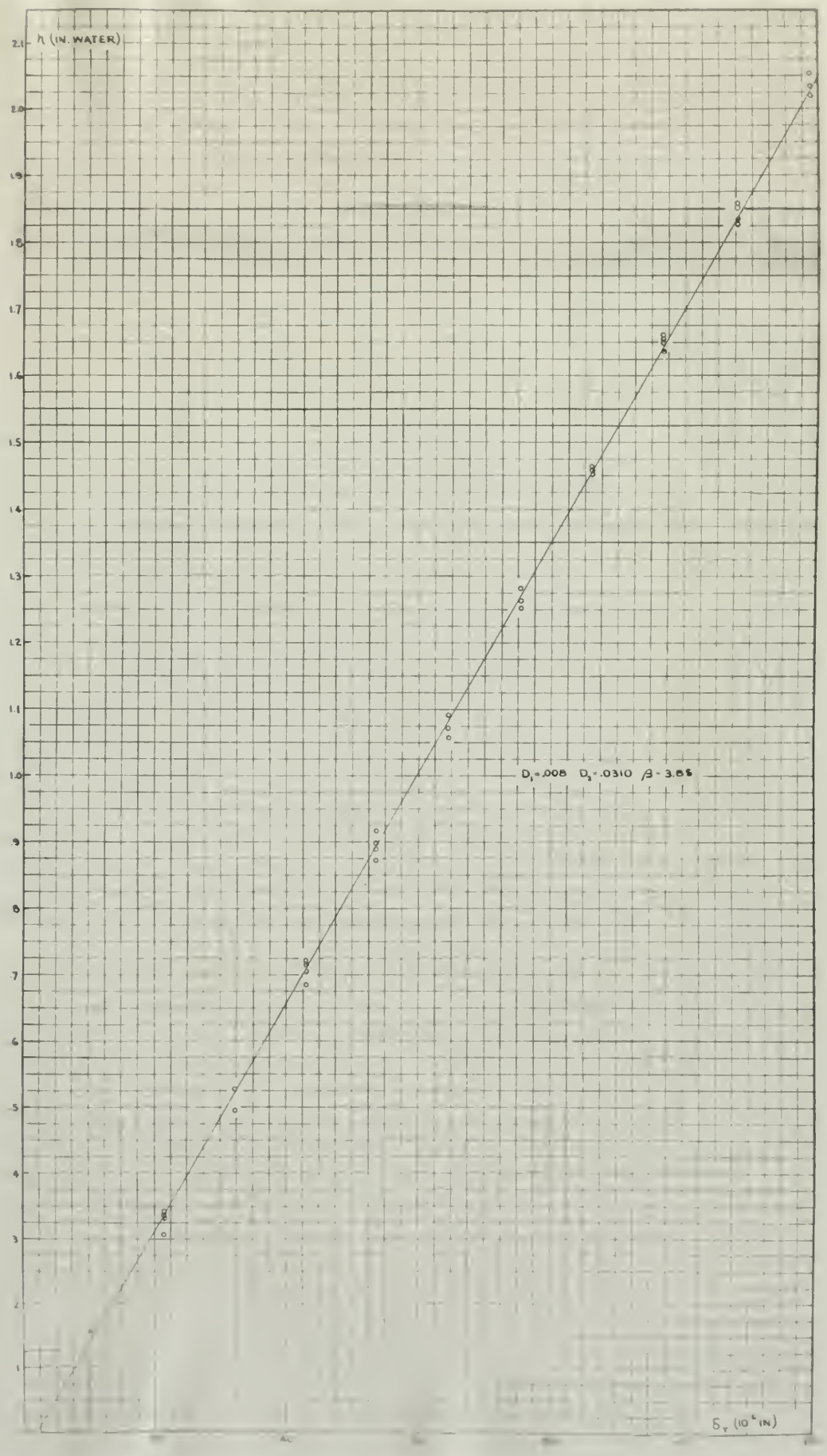

Figure 14c - Calibration curve, Combination C.

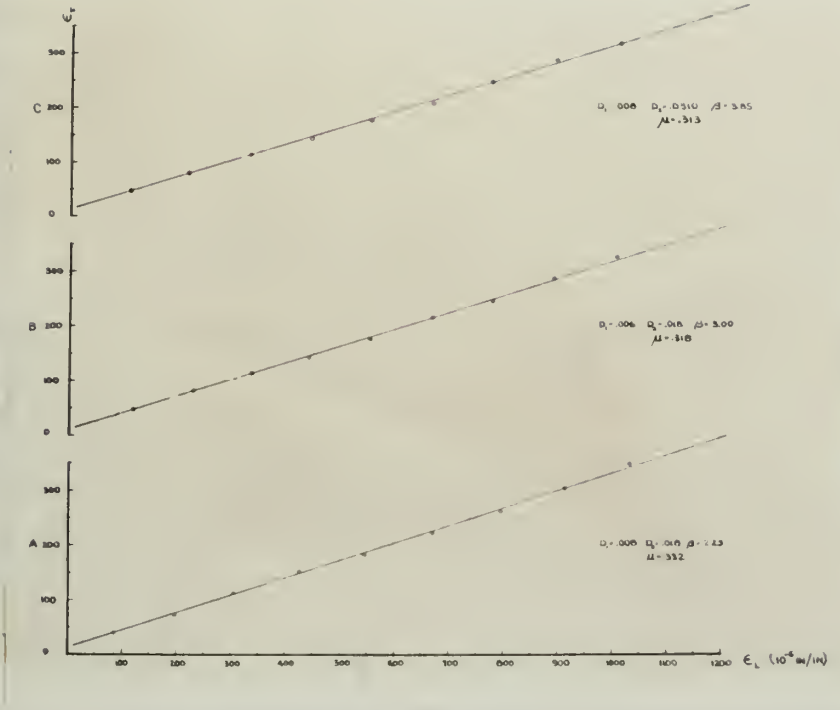

Figure 15 - μ curve

III TEST RESULTS AND COMMENTS

1 - Magnification

The magnification inherent to each combination tested is obtained from the slope of the calibration curve. In the case of combinations A and C which are plotted as straight lines, the magnification remained constant. Combination B was parabolic, but so nearly straight that little error is introduced if the slope of the extremes of this curve are taken. In fact by taking the extremes for slope determination, the magnification obtained is on the pessimistic side of the maximum realizable.

The tabulation below lists the magnifications obtained during test, along with those values predicted by Figure 3. Inasmuch as Figure 3 was designed only to give an estimate, the results obtained compare favorably with the actual M_s.

$\Delta s = 10^{-4}$

Combination or Curve	D_1	D_2	β	M_s Fig.3 Min.	M_s Fig.3 Max.	M_s Actual	Max. P.C. Difference
A	.008	.0180	2.25	11,800	12,300	13,400	-11.2
B	.006	.0180	3.00	20,000	21,600	18,500	16.6
C	.008	.0310	3.85	18,800	20,900	17,000	22.9

The tabulation above verifies the theory (page 8) in predicting effects of changing orifice siz es. From this table it can be seen that: -

a. M_s increases with increase in D_2.

b. M_s increases with decrease in D_1.

2 - Sensitivity

Since it has been estimated that the manometric column water level can be read to the nearest .01 cm. or .004", then the sensitivity of the strain ga ge is equal to the sensitivity in reading the manometer divided by the magnification.

Combination	Operation	ω
A	.004/13,400	3.0×10^{-7} inches
B	.004/18,500	2.2×10^{-7} inches
C	.004/17,000	2.4×10^{-7} inches

3 - Error in Using the Pneumatic Strain Gage

This error is an accumulation of errors that appear throughout the entire process of calibration and wire strain measurements. It includes:

a. Error in centering gage

This error affects the mechanical advantage built into the gage and should be computed on that basis. Using micrometers for setting the calipers, which in turn centers the gage, it is apparent that the gage could be set off center a maximum of $\pm$ .001". This would vary the mechanical advantage from 1.996 to 2.004 which is an error of $\pm$ 4/2000 = $\pm$ .2%.

In moving the gage from the test wire to the calibrating pins, the same effect manifests itself and another $\pm$ .2% is gained.

In returning to the test wire after calibration, there should be no error in centering as long as the column reading repeats itself.

b. Error in random scattering of calibration run points

This error includes the error in setting the interference fringes to the cross-hair reference, reading the water column during calibration and changes in conditions during readings.

It is obtained by drawing in an envelope to the calibration run plotted points so as to include all points above and below the curve drawn.

The error is computed by taking the Δs deviation of upper and lower envelopes at the upper limit of the range calibrated and dividing by the corresponding s.

This error for the several combinations appears as follows:

Combination	Operation	P. C. Error
A	$\pm 4.4/100$	$\pm 4.4\%$
B	$\pm 1.25/100$	$\pm 1.25\%$
C	$\pm 2.5/100$	$\pm 2.5\%$

c. Error in reading water column during test of wire

It is probable that the maximum error in reading the column meniscus is about $\pm.005$ cm. or $\pm.00197$ inches per reading. Since the transverse deformation and corresponding column readings were linearly related, Δh is essentially constant. Values for this error appear as follows:

Combination	Operation	P. C. Error
A	$.00197/.0767$	2.57
B	$.00197/.0788$	2.50
C	$.00197/.0708$	2.78

d. Using calibration curve

Since the calibration curves were plotted with the same accuracy to which the interferometer and water column could be read, it is safe to assume there is no error in reading the curve.

The above mentioned errors accumulate in the following manner:

Operation	Error Type	Combination A	B	C
1. Setting gage on test wire.	Centering	.40	.40	.40
2. Setting gage on calibrator.	Centering	.40	.40	.40
3. Calibration	Random Scattering.	8.80	2.50	5.00
4. Resetting gage on test wire	Reading Manometer.	2.57	2.50	2.78
	P. C. Error Σ	12.17	5.80	8.58

4 - Error in Determination of μ

Since $\mu = \frac{\epsilon_T}{\epsilon_L}$, the error appearing from division is the summation of the percent error determined for the pneumatic gage and the error characteristic of the Tuckerman strain gage. Tabulated, this appears as:

Combination	Error in ϵ_T	Error in ϵ_L	Error in μ
A	12.17	.2	12.37
B	5.80	.2	6.00
C	8.58	.2	8.78

If we use Figure 15 to read values of μ it must be realized that the curve plotted already has the error due to random scattering included in it, since the calibration curve was used to make up the plot of this figure.

Drawing in the envelopes on the μ curve plot and determining the range of possible straight line slopes within this band, we will then have the random scattering effect from all sources. In effect this is taking the $\pm$ $\Delta\mu$'s possible within the band and dividing by the plotted μ. For each combination, this error appears as follows:

Combination	Operation	P. C. Error
A	$.010/.332$	3.0
B	$.008/.318$	2.5
C	$.006/.313$	1.9

Values of μ determined by the three combinations are tabulated below:

Combination	μ
A	.332
B	.318
C	.313

5 - Reliability

Perhaps one of the most interesting results obtained during the test was that of Figure 16 which shows a comparison between the values of transverse deformation obtained with the three combinations.

W hen one considers the many operations involved in arriving at the final deformation readings obtained, it is remarkable that such close agreement is attained.

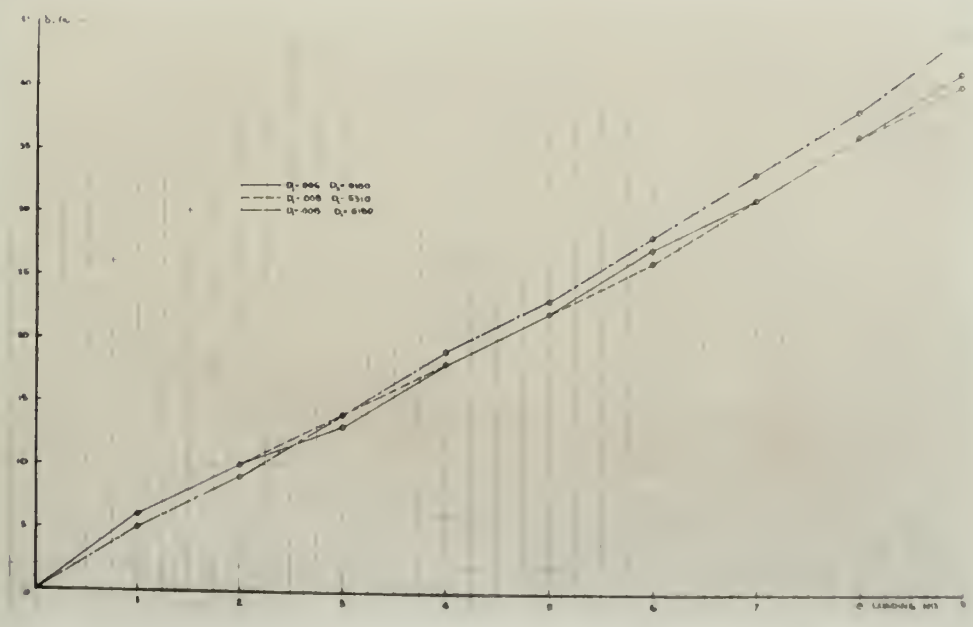

Figure 16 - Reliability of calibrating and wire testing arrangement.

6 - Duplication of Calibration Runs

Combination B was arbitrarily chosen and second calibration run made at a period of one week after the original run. The results of this run appear as Table VIII in the Appendix. The data obtained was plotted as $\triangle$'s on Figure 14b and indicates very little deviation from the actual calibration. This is another indication of gage and calibration a rrangement reliability.

7 - Recommendations for Improving Testing Efficiency

a. Design and fabricate a worm drive for the interferometer micrometer hand-wheel. With such an arrangement, the error in setting interference fringes could be entirely eliminated.

b. Design vibration absorbers for mounting entire test a rrangement. Errors would be considerably reduced.

c. Thread used on nozzle holder was sloppy and too coarse. Much time could be saved by correcting this condition.

d. All followers and orifice tip stops should be lapped and squared to greater precision.

e. Fabricate a larger loading bucket for tension producer. Range of use would be increased and with more data, results would be better. (Don't neglect permeability of lead shot in arriving at bucket capacity.)

f. "Solex" should be all metal instead of glass. The danger of breakage slowed work considerably.

g. Some consideration could be given to an improved centering device. Such a feature would save time in setting as well as eliminate the centering error.

h. Addition of a greater mechanical advantage to the tension producer lead screw drive. Great care had to be exercised in leveling the beam with the existing ratchet wrench so as to avoid jerky motion. It is felt that jerky motion was mainly responsible for erratic Tuckerman readings using combination "A" in particular (note Table V). This

condition may have been responsible for the variation of μ, obtained using this combination, from the other two combinations.

i. Perhaps the most important factor that must be given consideration is "Technique." It can't be overemphasized, that the quality of results depends so greatly on the procedure followed and in duplicating a good procedure once set up. It has been said that a good machinist can get good results using the crudest of equipment. It is believed that this same axiom holds true in making a test such as this one.

BIBLIOGRAPHY

1. Kiefer, P. J. and Kinney, G. F. Principles of Engineering Thermodynamics. Unpublished edition.

2. Lee, G. H. An Introduction to Experimental Stress Analysis. John Wiley & Sons, Inc. 1950.

3. Leiris, H. D. Sur la mesurue des constantes elastiques par amplification pneumatique des deformations. Seventh International Congress for Applied Mechanics, 1948.

4. Linford, A . Flow Measurements and Meters. E. and F. N. Spon. Ltd. 1949.

APPENDIX A

A - Development of Flow Equation

The development of the general theoretical flow equation is first taken up and then certain modifications are incorporated as a result of assumptions that are characteristic of the application for which it is being used.

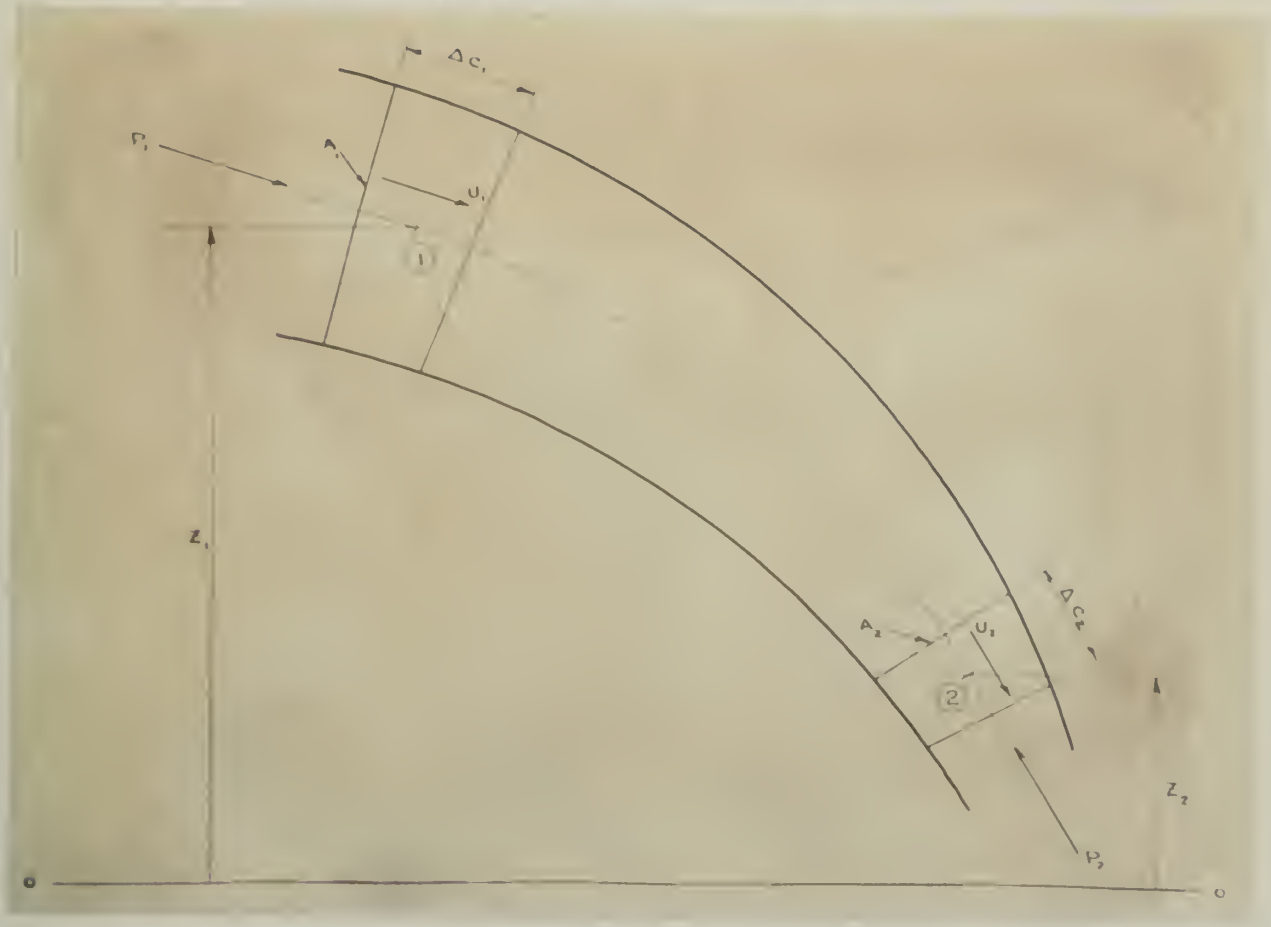

Figure 17 - Mechanics of flow

Referring to Figure 17 which represents a duct carrying fluid through a changing cross section, we see that, for the case of a compressible fluid as air, the work done in moving the fluid increment m from 1 to 2 is equal to the kinetic energy in passing it from 1 to 2. Since the density ρ is not constant, the volume V of the mass m is not constant.

Then $\text{Work}_{1-2} = \text{K.E.}_{1-2}$

$$\int_{P_2}^{P_1} V\,dP + (z_1 - z_2)mg = \frac{1}{2}mU_2^2 - \frac{1}{2}mU_1^2 \qquad (a)$$

The expansion is adiabatic since the pressure drop is rapid. Therefore, the equation defining the expansion can be written:

$$PV^K = P_1V_1^K = P_2V_2^K \qquad (b)$$

or

$$V = V_1\left(\frac{P_1}{P_2}\right)^{\frac{1}{K}}$$

and

$$\int_{P_2}^{P_1} V\,dP = V_1\int_{P_2}^{P_1}\left(\frac{P_1}{P}\right)^{\frac{1}{K}}dP \qquad (c)$$

(c) becomes when integrated:

$$\int V\,dP = V_1P_1^{1/K}\int_{P_2}^{P_1}\frac{dP}{P^{1/K}}$$

$$= \frac{V_1P_1^{1/K}}{1-K}\left[P^{1-\frac{1}{K}}\right]_{P_2}^{P_1}$$

$$= \frac{K}{K-1}V_1P_1^{1/K}\left(P_1^{\frac{K-1}{K}} - P_2^{\frac{K-1}{K}}\right)$$

$$= V_1P_1^{1/K}\left(\frac{K}{K-1}\right)\left[1-\left(\frac{P_2}{P_1}\right)^{\frac{K-1}{K}}\right]P_1^{\frac{K-1}{K}}$$

$$= P_1V_1\left(\frac{K}{K-1}\right)\left[1-\left(\frac{P_2}{P_1}\right)^{\frac{K-1}{K}}\right]$$

And the left side of equation (a) becomes, if we assume pressure taps $\underline{P}_1$ and $\underline{P}_2$ are on the same level so that $mg\,(z_1 - z_2) = 0$.

$$\int_{P_2}^{P_1} V\,dP = P_1V_1\left(\frac{K}{K-1}\right)\left[1-\left(\frac{P_2}{P_1}\right)^{\frac{K-1}{K}}\right] \qquad (d)$$

Now since $V_1 = \frac{m}{\rho_1}$ and $V_2 = \frac{m}{\rho_2}$

(b) becomes $P_1\left(\frac{m}{\rho_1}\right)^K = P_2\left(\frac{m}{\rho_2}\right)^K$

or $$\frac{\rho_1}{\rho_2} = \left(\frac{P_1}{P_2}\right)^{1/k} \qquad (e)$$

Further, mass continuity requires that

$$U_2 A_2 \rho_2 = U_1 A_1 \rho_1 \qquad (f)$$

or $$Q_2 \rho_2 = Q_1 \rho_1$$

Rearranging (f) and substituting (e), we have

$$U_2 = \frac{\rho_1}{\rho_2} \cdot \frac{A_1}{A_2} \cdot U_1$$

$$= \left(\frac{P_1}{P_2}\right)^{\frac{1}{k}} \cdot \frac{A_1}{A_2} \cdot U_1 \qquad (g)$$

And the right side of equation (a) becomes

$$\tfrac{1}{2} m (U_2^2 - U_1^2) = \tfrac{1}{2} m U_1^2 \left[\left(\frac{P_1}{P_2}\right)^{\frac{2}{k}} \frac{A_1^2}{A_2^2} - 1\right] \qquad (h)$$

Equating (d) and (h),

$$P_1 V_1 \left(\frac{k}{k-1}\right)\left[1 - \left(\frac{P_2}{P_1}\right)^{\frac{k-1}{k}}\right] = \tfrac{1}{2} m U_1^2 \left[\left(\frac{P_1}{P_2}\right)^{\frac{2}{k}} \left(\frac{A_1}{A_2}\right)^2 - 1\right] \qquad (i)$$

Recalling that $V_1 = \frac{m}{\rho}$ and placing $P_1 = \rho_1 g'$ as defined in the notation we have upon substituting into (i) and solving for U_1.

$$U_1 = \sqrt{2g'} \sqrt{\frac{P_1}{\rho}} \frac{\sqrt{\frac{k}{k-1}\left[1 - \left(\frac{P_2}{P_1}\right)^{\frac{k-1}{k}}\right]}}{\sqrt{\left(\frac{P_1}{P_2}\right)^{\frac{2}{k}} \left(\frac{A_1}{A_2}\right)^2 - 1}}$$

Again since $M' = Q_1 \rho_1 = A_1 U_1 \rho_1$

$$M' = A_1 \sqrt{2g'} \sqrt{P_1 \rho_1} \frac{\sqrt{\frac{k}{k-1}\left[1 - \left(\frac{P_2}{P_1}\right)^{\frac{k-1}{k}}\right]\left[\frac{P_2}{P_1}\right]^{\frac{2}{k}}}}{\sqrt{1 - \left(\frac{A_2}{A_1}\right)^2 \left(\frac{P_2}{P_1}\right)^{2/k}}}$$

Or simplifying and letting $C_u = \frac{1}{\sqrt{1 - \left(\frac{A_2}{A_1}\right)^2 \left(\frac{P_2}{P_1}\right)^{2/k}}}$

which is a correction for initial velocity, we have

$$M' = 8.02 C_v A_1 \sqrt{P_1 \rho_1} \sqrt{\frac{K}{K-1}\left[\left(\frac{P_2}{P_1}\right)^{\frac{2}{K}} - \left(\frac{P_2}{P_1}\right)^{\frac{K+1}{K}}\right]} \qquad (j)$$

Due to the fluid under consideration being a gas, it is apparent that the change in kinetic energy is accompanied by random motion of the gas particles, giving rise to turbulence. With turbulence, viscosity effects can be considered negligible. However, there are friction and eddy loss effects present which must be taken into account by a discharge coefficient C_D. Equation (j) then becomes finally:

$$M' = 8.02 A_1 C_v C_D \sqrt{P_1 \rho_1} \sqrt{\frac{K}{K-1}\left[\left(\frac{P_2}{P_1}\right)^{\frac{2}{K}} - \left(\frac{P_2}{P_1}\right)^{\frac{K+1}{K}}\right]} \qquad (k)$$

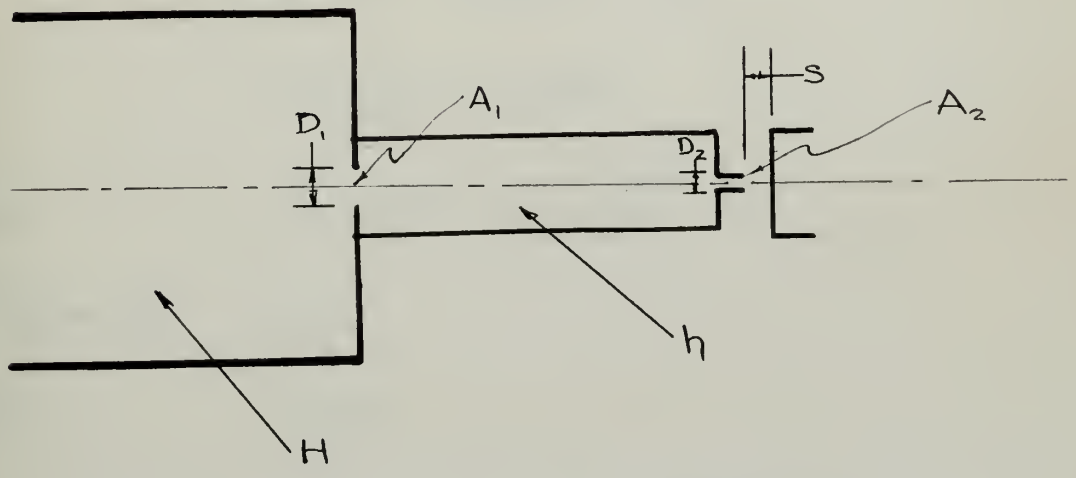

Figure 18 - Simple flow system.

Equation (k) applied to the system of Figure 18 becomes:

$$A_1 C_{v1} C_{D1} \sqrt{H \rho_1} \sqrt{\frac{k}{k-1}\left(\left[\frac{h}{H}\right]^{\frac{2}{k}} - \left[\frac{h}{H}\right]^{\frac{k+1}{k}}\right)} =$$

$$= A_2 C_{v2} C_{D2} \sqrt{h \rho_2} \sqrt{\frac{k}{k-1}\left(\left[\frac{ATM}{h}\right]^{\frac{2}{k}} - \left[\frac{ATM}{h}\right]^{\frac{k+1}{k}}\right)} \qquad (1)$$

Now if both $\underline{A_1}$ and $\underline{A_2}$ are sharp edge orifices, the variation between $\underline{C}_{D1}$ and $\underline{C}_{D2}$ will not be great, and it is legitimate to assume $\underline{C}_{D1} = \underline{C}_{D2}$.

By making the approach cross section large in comparison with $\underline{A_1}$ and the duct leading to $\underline{A_2}$ large in comparison with $\underline{A_2}$, it can be seen that the gas in the approach and in the duct leading to $\underline{A_2}$ can be considered in a stagnate state, and that the correction for initial velocity can be neglected.

Further, by using low pressures such that

$$\frac{H-h}{H} \text{ and } \frac{h-ATM}{h} \leq .01$$

$$\sqrt{\frac{k}{k-1}\left[\left(\frac{h}{H}\right)^{\frac{2}{k}} - \left(\frac{h}{H}\right)^{\frac{k+1}{k}}\right]}$$

and $$\sqrt{\frac{k}{k-1}\left[\left(\frac{ATM}{h}\right)^{\frac{2}{k}} - \left(\frac{ATM}{h}\right)^{\frac{k+1}{k}}\right]}$$

reduces to $$\sqrt{\frac{H-h}{H}}$$

and $$\sqrt{\frac{h-ATM}{h}}$$

respectively.

(within .5 percent error in accuracy of results)

Again, with low pressures, the variation in density of the flowing gas in the duct and atmosphere will be negligible, and we can reduce (1) to

$$A_1 \sqrt{H-h} = A_2 \sqrt{h-ATM}$$

or by using gage pressure (m)

$$A_1\sqrt{H-h} = A_2\sqrt{h}$$

Solving for h we have

$$h = \frac{H}{1+\left(\frac{A_2}{A_1}\right)^2} \qquad (n)$$

Since $A_1 = \frac{\pi D_1^2}{4}$ and $A_2 = \pi D_2 S$

$$h = \frac{H}{1+\frac{16 D_2^2 S^2}{D_1^4}} \qquad (1)$$

APPENDIX B

TABLE III - Figure 3 Computations; D_1 =.001"; H =8.303"H_2O

$\alpha \times 10^{-4}$	$-32\beta\alpha H$	$\alpha^2 \times 10^{-6}$	$16\beta^2\alpha^2 \times 10^{-2}$	$(1+16\beta^2\alpha^2)^2$	$\frac{dh}{d\alpha}$	$\frac{dh}{ds} \times 10^3$	$s \times 10^{-6}$
			β = 8.00				
10	1090	1	6.55	1.117	977	122.0	8
20	2180	4.00	26.20	1.595	1367	170.8	16
Max. 22.6	2460	5.12	33.50	1.785	1380	172.8	17.92
25	2720	6.25	40.90	1.990	1367	170.8	20
30	3270	9.00	59.00	2.530	1290	161.2	24
			β = 7.5				
15	1262	2.25	11.4	1.245	1014	135.2	11
25	2104	6.25	31.7	1.735	1215	162.0	19
M 25.7	2162	6.62	33.6	1.784	1215	1620	19.28
30	2530	9.00	45.7	2.120	1193	159.2	23
35	2942	12.30	62.4	2.650	1112	148.4	26
			β = 7.0				
15	965	2.25	8.67	1.140	847	120.9	11
25	1607	6.25	24.10	1.542	1041	148.8	18
M 29.5	1896	8.71	33.60	1.785	1062	151.6	21
35	2250	12.30	47.4	2.180	1032	147.6	25
40	2570	16.00	61.7	2.620	980	140.0	28
			β = 6.5				
25	1200	6.25	18.0	1.398	858	132.0	16
30	1440	9.00	25.9	1.585	908	139.6	20
M 34.1	1638	11.62	33.4	1.782	918	141.2	22
40	1920	16.00	46.0	2.130	902	138.8	26
45	2160	20.30	58.4	2.520	857	131.6	29
			β = 6.0				
30	1038	9.0	18.7	1.410	737	122.8	18
35	1212	12.30	25.6	1.580	768	128.0	21
M 40.2	1390	16.20	33.7	1.782	780	130.0	24
45	1559	20.30	41.8	2.020	772	128.8	27
50	1730	25.00	52.0	2.320	746	124.4	30

TABLE III (continued-page 2) D_1 =.001"; H =8.303"H_2O

	$\alpha \times 10^{-4}$	$-32\beta^4\alpha H$	$\alpha^2 \times 10^{-6}$	$16\beta^4\alpha^2 \times 10^{-2}$	$(1+16\beta^4\alpha^2)^2$	$\frac{dh}{d\alpha}$	$\frac{dh}{ds} \times 10^3$	$s \times 10^{-6}$
				$\beta = 5.5$				
	40	980	16.00	23.5	1.530	641	116.4	22.0
	45	1103	20.30	29.8	1.682	657	119.3	25
Max.	47.7	1169	22.80	33.6	1.782	656	119.2	26
	50	1225	25.00	36.8	1.871	653	118.8	28
	55	1349	30.30	44.6	2.090	645	117.2	30
				$\beta = 5.0$				
	45	750	20.30	20.3	1.455	516	103.2	22.5
	55	917	30.30	30.3	1.706	538	107.6	27.5
M	57.8	965	33.50	33.5	1.782	542	108.2	28.9
	60	1000	36.00	36.0	1.854	539	107.6	32.5
	82	1365	67.40	67.5	2.820	484	96.8	41.0
				$\beta = 4.5$				
	40	440	16.0	10.6	1.220	361	72.0	20
	65	715	42.3	28.0	1.640	436	96.8	29
M	71.2	783	50.8	33.6	1.782	439	97.6	32
	75	830	56.3	37.2	1.890	439	97.6	34
	90	990	81.0	53.5	2.36	419	93.2	41
				$\beta = 4.0$				
	70	478	49.0	20.2	1.446	331	82.8	28
	85	580	72.3	29.6	1.680	345	86.2	34
M	90.3	616	81.8	33.3	1.780	346	86.5	36
	95	648	90.3	37.0	1.880	345	86.2	38
	110	750	121.0	49.5	2.240	334	83.5	44
				$\beta = 3.5$				
	80	324	64	15.6	1.340	242	69.2	28
	110	445	121	29.4	1.680	265	75.7	39
M	117.5	475	138	33.7	1.785	226	76.0	41
	120	486	144	35.0	1.825	266	76.0	42
	150	607	225	54.7	2.390	254	72.6	53
				$\beta = 3.0$				
	120	259	144	18.7	1.410	184	61.3	36
	150	324	225	29.2	1.678	193	64.3	45
M	160.5	347	256	33.2	1.780	195	65.0	48
	170	367	290	37.6	1.895	194	64.7	51
	200	432	400	51.9	2.310	187	62.3	60

TABLE III (continued-page 3) D_1 =.001"; H =8.303"H_2O

	$\alpha \times 10^{-4}$	$-32\beta^4\alpha H$	$\alpha^2 \times 10^{-6}$	$16\beta^4\alpha^2 \times 10^{-2}$	$(1+16\beta^4\alpha^2)^2$	$\frac{db}{d\alpha}$	$\frac{dh}{ds}$	$s \times 10^{-6}$
				$\beta = 2.5$				
	16	167	256	16.0	1.352	124	49.6	40
	21	219	441	27.6	1.630	135	54.0	53
Max	23.1	241	535	33.6	1.782	135	54.0	58
	25	261	625	39.2	1.941	134	53.6	63
	30	313	900	56.5	2.460	123	49.2	75
				$\beta = 2.4$				
	17	152	290	15.6	1.340	113	43.1	41
	23	205	530	28.4	1.653	124	51.6	55
M	25	223	625	33.5	1.782	126	52.5	60
	27	241	730	39.2	1.940	124	51.6	65
	33	295	1090	58.4	2.520	117	48.7	79
				$\beta = 2.3$				
	16	121	256	11.5	1.246	97	42.1	37
	24	180	578	26.1	1.596	113	49.2	55
M	27.3	205	748	33.7	1.788	115	50.0	63
	30	226	900	40.6	1.980	114	49.6	69
	38	286	1446	65.2	2.740	105	45.4	87
				$\beta = 2.2$				
	15	94	225	8.5	1.180	80	36.3	33
	25	157	625	23.5	1.530	103	46.6	55
M	29.8	187	890	33.5	1.782	105	47.7	66
	35	219	1230	46.3	2.140	102	46.6	77
	45	282	2030	76.4	3.120	90	41.1	99
				$\beta = 2.1$				
	15	78	225	7.1	1.153	68	32.2	32
	25	131	625	19.6	1.432	91	43.2	53
M	32.6	170	1065	33.4	1.782	96	45.6	69
	35	183	1230	38.6	1.922	95	45.3	74
	45	235	2030	63.6	2.680	91	43.4	95
				$\beta = 2.0$				
	20	85	400	10.25	1.220	70	34.9	40
	30	128	900	23.02	1.520	84	42.1	60
M	36.1	154	1310	33.50	1.782	86	43.2	72
	40	171	1600	41.00	1.995	86	42.8	80
	50	213	2500	64.00	2.695	79	39.6	100

TABLE III (continued-page 4) D_1 =.001"; H =8.303"H_2O

	$\alpha^{\times 10^{-4}}$	$-32\beta^4\alpha H$	$\alpha^{2\times 10^{-6}}$	$16\beta^4\alpha^{2\times 10^{-2}}$	$(1+16\beta^4\alpha^2)^2$	$\frac{dh}{d\delta}$	$\frac{dh}{ds}^{\times 10^{-5}}$	$s^{\times 10^{-6}}$
				$\beta = 1.9$				
	15	52	225	4.69	1.095	47.6	25.0	29
	35	122	1230	25.62	1.580	76.9	40.5	67
Max.	40	139	1600	33.40	1.782	77.9	41.0	76
	45	156	2030	42.40	2.030	76.8	40.4	86
	65	226	4230	88.30	3.560	63.5	33.4	124
				$\beta = 1.8$				
	25	71	625	10.60	1.220	57.8	32.1	45
	35	99	1230	20.82	1.460	67.8	37.7	63
M	46	130	2120	36.00	1.855	70.2	39.0	83
	50	141	2500	42.30	2.030	70.1	39.0	90
	60	170	3600	61.10	2.600	65.2	36.2	108
				$\beta = 1.7$				
	20	45	400	5.38	1.115	40.3	23.8	34
	40	90	1600	21.50	1.480	60.7	35.7	68
M	49.8	112	2480	33.40	1.781	62.8	36.9	85
	60	135	3600	48.60	2.210	60.9	35.8	102
	80	179	6400	86.30	3.480	51.5	30.3	136
				$\beta = 1.6$				
	35	61	1230	12.92	1.276	48.1	30.1	56
	50	88	2500	26.25	1.600	54.8	34.3	80
M	56.4	99	3180	33.40	1.782	55.3	34.6	90
	60	105	3600	37.80	1.910	55.0	34.4	96
	75	131	5630	59.20	2.540	51.7	32.3	120
				$\beta = 1.5$				
	40	54	1600	13.00	1.280	41.3	27.6	60
	60	81	3600	29.30	1.680	48.4	32.2	90
M	64.2	87	4125	33.50	1.782	48.8	32.5	96.2
	70	95	4900	39.80	1.958	48.5	32.3	105
	90	122	8100	65.90	2.760	44.2	29.4	135

TABLE IV - Calibration Data; * D_1 =.008"; D_2 =.0180"

h	Δh	h	Δh	h	Δh	h	Δh
28.00		28.00		28.00		28.00	
27.64	.36	27.64	.36	27.64	.36	27.65	.35
27.27	.37	27.28	.36	27.30	.34	27.29	.36
26.87	.40	26.90	.38	26.95	.35	26.92	.37
26.50	.37	26.50	.40	26.60	.35	26.55	.37
26.12	.38	26.09	.41	26.24	.36	26.16	.39
25.77	.35	25.73	.36	25.86	.38	25.80	.36
25.39	.38	25.35	.38	25.50	.36	25.43	.37
25.03	.36	24.98	.37	25.15	.35	25.08	.35
24.67	.36	24.64	.34	24.82	.33	24.73	.35
24.30	.37	24.32	.32	24.44	.38	24.36	.37
23.94	.36	24.00	.32	24.11	.33	24.00	.36
				D_1 =.006";		D_2 =.0180"	
27.09		27.09		27.09		27.09	
26.66	.43	26.60	.49	26.61	.48	26.63	.46
26.06	.60	26.02	.58	26.06	.55	26.05	.58
25.50	.56	25.48	.54	25.50	.56	25.48	.57
24.95	.55	24.98	.50	24.97	.53	24.93	.55
24.41	.54	24.45	.53	24.44	.53	24.41	.52
23.93	.48	23.95	.50	23.93	.51	23.93	.48
23.40	.53	23.46	.49	23.44	.49	23.43	.50
22.95	.45	23.00	.46	22.97	.47	22.98	.45

* All readings in centimeters.

TABLE IV (continued-page 2)* D_1 =.008"; D_2 =.0310"

h	Δh	h	Δh	h	Δh	h	Δh
29.97		29.97		29.97		29.97	
29.58	.39	29.56	.41	29.58	.39	29.57	.40
29.19	.39	29.10	.46	29.13	.45	29.12	.45
28.71	.48	28.63	.47	28.63	.50	28.63	.49
28.23	.48	28.18	.45	28.14	.49	28.15	.48
27.75	.48	27.71	.47	27.64	.50	27.67	.48
27.28	.47	27.25	.46	27.20	.44	27.20	.47
26.79	.49	26.76	.49	26.72	.48	26.72	.48
26.25	.54	26.28	.48	26.26	.46	26.25	.47
25.78	.47	25.81	.47	25.77	.49	25.75	.50
25.31	.47	25.33	.48	25.26	.51	25.25	.50
24.80	.51	24.84	.49	24.75	.51	24.75	.50
24.35	.45	24.39	.45	24.25	.50	24.26	.49
23.92	.43	23.96	.43	23.82	.43	23.81	.45
23.56	.36	23.54	.42	23.36	.46	23.36	.45
23.25	.31	23.22	.32	23.03	.33	23.00	.36

* All readings in centimeters.

TABLE V - Deformation of Wire Data;

Tuckerman Correction
#855: 2.009 x 1.003
#850: 1.987 x 1.003

D_1 =.008"; D_2 =.018"

Tuckerman 855	Tuckerman 850	h	△h	Load
11.32	10.88	28.00		4#
10.80	10.26	27.84	.16	6
10.29	9.68	27.69	.15	8
9.77	9.09	27.54	.15	10
9.20	8.47	27.38	.16	12
8.62	7.86	27.22	.16	14
8.01	7.22	27.05	.17	16
7.41	6.59	26.87	.18	18
6.83	5.97	26.69	.18	20
6.25	5.36	26.51	.18	22

D_1 =.008"; D_2 =.0310"

14.42	11.81	29.97		4
13.91	11.22	29.81	.16	6
13.40	10.66	29.63	.18	8
12.86	10.05	29.46	.17	10
12.34	9.45	29.28	.18	12
11.79	8.90	29.09	.19	14
11.22	8.32	28.90	.19	16
10.67	7.76	28.71	.19	18
10.08	7.16	28.51	.20	20
9.50	6.57	28.32	.19	22

D_1 =.006"; D_2 =.0180"

14.20	11.82	27.09		4
13.70	11.14	26.89	.20	6
13.19	10.56	26.67	.22	8
12.68	10.00	26.47	.20	10
12.13	9.48	26.24	.23	12
11.56	8.92	26.01	.23	14
11.01	8.34	25.79	.22	16
10.46	7.76	25.55	.24	18
9.90	7.18	25.31	.24	20
9.34	6.60	25.08	.23	22

NOTE: h readings in centimeters

TABLE VI - Tabulation of Calibration and μ Curve Equations

CALIBRATION

Combination	Straight Line	Parabola
D_1=.008 D_2=.0180	h=.3673S-.0118	h=-.0019s^2+.3886s-.0495
D_1=.006 D_2=.0180	h=.5225s	<u>h=-.0081s^2+.5927s-.1107</u>
D_1=.008 D_2=.0310	<u>h=.4747s-.0987</u>	h=-.0006s^2+.4826s-.1125

μ CURVES

Combination	Straight Line
D_1=.008 D_2=.0180	ϵ_T =.3197 ϵ_L + 13
D_1=.006 D_2=.0180	ϵ_T =.3094 ϵ_L + 9
D_1=.008 D_2=.0310	ϵ_T =.2992 ϵ_L + 14

NOTE: Equations used underlined.

TABLE VII - Transverse and Longitudinal Strains

Tuckerman 855-Corr.	Tuckerman 850-Corr.	Mean 855+850	$\Delta\epsilon_t$	$\epsilon_t \times 10^{-4}$ (in)	h(cm)	h(in)	s-cal. (curve)	ϵ_r:- s/Dwire
		D_1=.008" D_2=.0180"						
22.28	21.68	21.98		0	0	0	0	0
21.76	20.45	21.11	.87	.87	.16	.063	5	40
20.73	19.29	20.01	1.10	1.97	.31	.122	9	72
19.69	18.12	18.92	1.09	3.06	.46	.181	14	112
18.54	16.88	17.71	1.21	4.27	.62	.244	19	152
17.37	15.67	16.52	1.19	5.46	.78	.307	23	184
16.14	14.39	15.27	1.25	6.71	.95	.374	28	224
14.93	13.13	14.03	1.24	7.95	1.13	.445	33	264
13.76	11.90	12.83	1.20	9.15	1.31	.516	38	304
12.59	10.68	11.64	1.19	10.34	1.49	.587	44	352
		D_1=.008" D_2=.0310"						
29.06	23.54	26.30		0	0	0	0	0
28.03	22.36	25.20	1.10	1.10	.16	.063	6	48
27.00	21.25	24.13	1.07	2.17	.34	.134	10	80
25.91	20.03	22.97	1.14	3.31	.51	.201	14	112
24.87	18.83	21.85	1.12	4.43	.69	.272	18	144
23.76	17.74	20.75	1.10	5.53	.88	.346	22	176
22.61	16.58	19.60	1.15	6.68	1.07	.421	26	208
21.50	15.47	18.49	1.11	7.79	1.26	.496	31	248
20.31	14.27	17.29	1.20	8.99	1.46	.575	36	288
19.14	13.09	16.12	1.17	10.16	1.65	.650	40	320
		D_1=.008" D_2=.0310"						
28.61	23.56	26.09		0	0	0	0	0
27.61	22.20	24.90	1.19	1.19	.20	.079	6	48
26.58	21.05	23.82	1.08	2.27	.42	.165	10	80
25.55	19.93	22.74	1.08	3.35	.62	.244	14	112
24.44	18.89	21.67	1.07	4.42	.85	.335	18	144
23.29	17.78	20.54	1.13	5.55	1.08	.425	22	176
22.19	16.62	19.41	1.13	6.68	1.30	.512	27	216
21.08	15.47	18.28	1.13	7.81	1.54	.606	31	248
19.95	14.31	17.13	1.15	8.96	1.78	.701	36	288
18.82	13.15	15.99	1.14	10.10	2.01	.791	41	328

TABLE VIII - Check on Calibration with D_1=.006", D_2=.0180"

h_1 (cm.)	Δh	h_2 (cm.)	Δh	h_1 (cm.)	h_2 (cm.)	h_1 (in.)	h_2 (in.)
27.09		27.09		0	0	0	0
26.60	.49	26.62	.47	.49	.47	.193	.185
26.07	.53	26.08	.54	1.02	1.01	.402	.398
25.52	.55	25.51	.57	1.57	1.58	.618	.622
25.00	.52	24.99	.52	2.09	2.10	.823	.827
24.47	.53	24.44	.55	2.62	2.65	1.031	1.043
23.98	.49	23.94	.50	3.11	3.15	1.224	1.240
23.49	.49	23.43	.51	3.60	3.66	1.417	1.440
23.02	.47	22.95	.48	4.07	4.14	1.602	1.630

	CENTER FLANGE SHEAVE	1	K-MONEL	NAVY SPECS 46 M 5J HOT ROLLED
	SHEAVE SUPPORT	1	MONEL	" " 46 M 7 PLUS .010-.02 STOCK
	[illegible]	1	↓	" "
	[illegible]	1	MILD STEEL	TURNED ONE PIECE [illegible]

ASSEMBL PIECES 1 & 2, CL 4 [illegible]
3 & 7, CL 5 RUNNING FIT
[illegible], CL 5, "
[illegible], CL 2, [illegible]
[illegible], CL 5, [illegible]
[illegible], CL 3, MEDIUM OR RUNNING FIT; + [illegible]

A | B